

University of Vermont

UVM ScholarWorks

Graduate College Dissertations and Theses

Dissertations and Theses

2024

Organic Fouling Mitigation In Forward Osmosis Technology Through The Use Of Oscilattig Alternating Current Electric Fields

Logan Werner
University of Vermont

Follow this and additional works at: <https://scholarworks.uvm.edu/graddis>



Part of the [Environmental Engineering Commons](#), and the [Water Resource Management Commons](#)

Recommended Citation

Werner, Logan, "Organic Fouling Mitigation In Forward Osmosis Technology Through The Use Of Oscilattig Alternating Current Electric Fields" (2024). *Graduate College Dissertations and Theses*. 1818. <https://scholarworks.uvm.edu/graddis/1818>

This Thesis is brought to you for free and open access by the Dissertations and Theses at UVM ScholarWorks. It has been accepted for inclusion in Graduate College Dissertations and Theses by an authorized administrator of UVM ScholarWorks. For more information, please contact schwrrks@uvm.edu.

ORGANIC FOULING MITIGATION IN FORWARD OSMOSIS TECHNOLOGY
THROUGH THE USE OF OSCILLATING ALTERNATING CURRENT ELECTRIC
FIELDS

A Thesis Presented

by

Logan Werner

To

The Faculty of the Graduate College

of

The University of Vermont

In Partial Fulfillment of the Requirements
for the Degree of Master of Science
Specializing in Civil and Environmental Engineering

January, 2024

Defense Date: October 25, 2023
Thesis Examination Committee:

Appala Raju Badireddy, Ph.D., Advisor
Amber Doiron, Ph.D., Chairperson
Matthew Scarborough, Ph.D.
Holger Hoock, DPhil, Dean of the Graduate College

Abstract

Forward osmosis (FO) is the term given to osmosis in water filtration applications. FO has many advantages to conventional membrane filtration processes. The lack of external pressure needed to force solvent through the membrane is dramatically decreased in FO, resulting in a lower cost of operation compared to reverse osmosis. Lower external pressures also result in decreased fouling on the membrane surface and improved permeate flux. Fouling is one of the foremost challenges within the membrane filtration industry and is one of the biggest contributors to operating costs. While FO results in less fouling than RO, fouling remains a major concern and results in significant expenses to operate FO. Many techniques exist to combat fouling, such as back washing, flushing, and chemical cleaning, however these techniques can be cost intensive and harmful to membrane integrity and performance. As a result, there is great interest in less intrusive cleaning techniques such as acoustic cleaning or electric fields that can be applied to mitigate fouling without compromising the membrane. Electric cleaning has shown great promise as an in-situ cleaning method, offering increased performance in membrane flux.

Electric field membrane cleaning involves applying an electric field perpendicular to the membrane surface, resulting in the movement of charged particles towards the electrodes at either side of the filtration channel, reducing the occurrence of fouling. Most electric field membrane cleaning techniques use a direct current (DC) electric field to cause this motion, called electroosmosis. DC cleaning has various drawbacks, such as electrolysis at the electrodes, corrosion of the electrodes, and further damage to the membrane surface which hinders DC cleaning performance. There is currently limited literature involving the use of alternating current (AC) fields for membrane cleaning. The aim of this study was to examine the feasibility of AC fields as an in-situ cleaning technique in FO application. Flux performance was assessed using bovine serum albumin (BSA) and sodium alginate as model foulants. Flux was measured over a 6 to 8-hour filtration period using a pulsed AC field applied every 2-hours, and a continuous AC field applied over the duration of filtration. Sodium chloride was used as a draw agent.

Results from these experiments indicate that AC electric fields are an effective method for in-situ organic fouling mitigation in FO process. Continuous and pulsed fields of various frequencies, conducted with foulant material in the feed solution, have demonstrated to improve flux retention to levels comparable to clean water flux conditions with no foulants. Normalized flux in the presence of foulants was raised from as low as 40% of initial flux at the conclusion of the trial to as high as 90% of initial flux with the application of electric field. Pulsed AC field application appeared to be more effective than continuous field, both in terms of fouling mitigation and lower energy input requirement.

Acknowledgments

I would firstly like to thank the Department of Civil and Environmental Engineering as well as Department of Urological Surgery at the University of Vermont Larner College of Medicine for financial and academic support throughout my graduate studies and the duration of this project. I would next like to thank my advisor, Dr. Appala Raju Badireddy, for his belief in me in taking on this project, for his constant and unwavering support throughout my academic career, and for his friendship and mentorship. I also would like to sincerely thank Dr. Richard Grunert, MD FACS and Dr. David Sobel, MD FACS for their support and guidance through this project, as well as their mentorship and assistance in undertaking this research project. Next, I would like to thank my committee members, Dr. Amber Doiron and Dr. Matthew Scarborough, for agreeing to serve as my chair members and for their guidance in delivering this report and presentation to the graduate college.

I would also like to extend a special thanks to Dr. Britt Holmen, who helped spark my passion for Environmental Engineering and helped to inspire me to be a dedicated engineer through her passion and friendship. I would also like to thank Dr. Holmen for helping me to believe in myself as a researcher. A big thanks also is extended to my research group and lab mates, notably Kamruzzaman (Sakib) Khan, Elliot Maker, Ryan Weinstein, and Yuxiang Shen, for their friendship and uplifting spirits during long nights in the lab. I also would like to acknowledge and sincerely thank the entire faculty of the Civil & Environmental Engineering, whose dedication to helping their students has helped me tremendously. I also would like to thank Pattie McNatt for all of her help in the

administrative aspects of graduate work and for putting up with my last-minute orders and requests.

Lastly and most importantly, I would like to make a special thank you to my parents, Dr. Leanna Lawter and Doug Werner, for helping me grow into the adult I am today, my grandparents, Poppy and Nana, who inspired me to undertake these studies in the first place and have constantly provided me with the encouragement and support I needed to complete my research, and Grandma Hope and Grandpa Rod, who are no longer with us but still inspired me to pursue my passions, my siblings, Emory Werner and Dalton Werner, for their support, and my friends, particularly Alexandra Swetland, who have always supported me and have kept me motivated.

Table of Contents

Acknowledgments	ii
List of Tables	vi
List of Figures	vii
Chapter 1: Introduction	1
1.1 Problem Statement	1
1.2 Summary of Research Contributions	4
1.3 Thesis Outline	5
Chapter 2: Literature Review	6
2.1 Forward Osmosis in Desalination and Fluid Recovery	6
2.2 Fouling in Forward Osmosis Technologies	7
2.3 Anti-Fouling Methods and Practices in Forward Osmosis	9
2.3.1 Traditional Practices	9
2.3.2 Electric Field Membrane Cleaning	11
2.4 Measuring Forward Osmosis Performance	12
Chapter 3. Testing Methods Employed in Research	14
3.1 Introduction	14
3.2 Testing Device	15
Chapter 4: Foulants, Feed and Draw Solution Composition, and Membrane Material	19
4.1 Introduction	19
4.2 Bovine Serum Albumin	19
4.3 Sodium Alginate	20
4.4 Feed Solutions	22
4.5 Draw Solution	23
4.6 Cellulose Triacetate Membrane	24
Chapter 5: Laboratory Methods to Induce Fouling	25
5.1 Introduction	25
5.2 Method Explored	25
5.3 Advantages and Limitations of the Method Explored	28
Chapter 6: Antifouling Experiments with Electric Field	29
6.1 Introduction	29
6.2 Results and Discussion	29

6.2.1 BSA Fouling in Absence of Electrolyte	29
6.2.2 BSA Fouling in Presence of Calcium Chloride Electrolyte	32
6.2.3 Alginate Fouling	36
6.3 Conclusions	41
Chapter 7: Membrane Characterization	45
7.1 Introduction	45
7.2 SEM Imaging	45
7.3 AFM Imaging	50
7.4 Fourier Transform Infrared (FTIR) Spectroscopy	50
7.5 Conclusions	57
Chapter 8: Conclusions	58
8.1 Summary of Data	58
8.2 Limitations in Research	59
8.3 Future Research Possibilities	59
Chapter 9: References	62

List of Tables

Table	Page
Table 1: Summary of composition of draw solutions used in this research.....	23

List of Figures

Figure	Page
Figure 1: Schematic of Forward Osmosis principle. Water from the feed solution permeated into the draw solution, diluting the draw solution.....	2
Figure 2: Comparison between fouling behaviors in Reverse Osmosis (RO) and Forward Osmosis (FO), demonstrating the effect of applied pressure on foulant layer. Higher applied pressures cause more severe fouling due to compaction of the fouling layer.....	8
Figure 3: Top view of filtration cell produced for use in this study.....	16
Figure 4: Side view of filtration cell produced for study, showing location of inlet and outlet ports.....	17
Figure 5: Schematic drawing of experimental set up. Feed solution (left) provides water to permeate into the draw solution (right). A power supply is connected to the electrodes, and the electric field is applied in the direction of permeating water, perpendicular to the membrane surface.....	18
Figure 6: Representation of the BSA molecule, obtained from the National Library of Medicine [42].....	20
Figure 7: Chemical structure of the sodium alginate molecule, obtained from the National Library of Medicine [45].....	21
Figure 8: Chemical structure of the sodium alginate molecule, obtained from the National Library of Medicine [61].....	24
Figure 9: Lab scale set up utilized for this research. Draw solution (left) is placed on a scale to monitor changes in volume. Feed solution (right) is continuously stirred to ensure the solution is well mixed.....	26
Figure 10: Normalized flux for BSA fouling conditions for 1 g/L concentration and no CaCl ₂ with 1 kHz 20 V _{p-p} electric field. Clean water (blue) experienced a 10% loss in initial flux. BSA fouling with no field (orange) lost 25% of flux performance over the course of the filtration. Continuous field (yellow) application in fouling conditions decreased the percentage of flux lost, with a 10% of flux loss over the duration of the trial. Pulsed field (grey) in fouling condition trials saw an improvement of flux performance compared to clean water, losing only 5% of flux over 8 hours.....	31

Figure 11: Normalized flux for BSA fouling conditions for 200 mg/L concentration and 0.5 mM CaCl ₂ at 100 Hz 20 V _{p-p} electric field. Clean water (blue) experienced a 10% loss in initial flux. BSA fouling with no field (orange) lost 19% of flux performance over the course of the filtration. Continuous field (green) application in fouling conditions decreased the percentage of flux lost, with a 11% of flux loss over the duration of the trial.....	33
Figure 12: Normalized flux for BSA fouling conditions for 200 mg/L concentration and 0.5 mM CaCl ₂ at 1 kHz 20 V _{p-p} electric field. Clean water (blue) experienced a 10% loss in initial flux. BSA fouling with no field (orange) lost 19% of flux performance over the course of the filtration. Continuous field (grey) application in fouling conditions decreased the percentage of flux lost, with a 9% of flux loss over the duration of the trial.....	34
Figure 13: Normalized flux for BSA fouling conditions for 200 mg/L concentration and 0.5 mM CaCl ₂ at 100 Hz 20 V _{p-p} electric field. Clean water (blue) experienced a 10% loss in initial flux. BSA fouling with no field (orange) lost 19% of flux performance over the course of the filtration. Continuous field (yellow) application in fouling conditions decreased the percentage of flux lost, with a 15% of flux loss over the duration of the trial.....	35
Figure 14: Normalized Flux for Alginate fouling conditions under a 100 Hz Field. Clean water (blue) lost 15% of flux during filtration. Alginate fouling with no field filtration (orange) lost up to 55% of flux. Continuous field application under Alginate fouling (grey) lost 19% of flux. Pulsed field application under alginate fouling (yellow) demonstrated similar performance to clean water filtration, losing 30% of flux throughout the trial.....	36
Figure 15: Normalized Flux for Alginate fouling conditions under a 1 kHz Field. Clean water (blue) lost 15% of flux during filtration. Alginate fouling with no field filtration (orange) lost up to 55% of flux. Continuous field application under Alginate fouling (grey) lost 24% of flux. Pulsed field application under alginate fouling (yellow) demonstrated similar performance to clean water filtration, losing 14% of flux throughout the trial.....	39
Figure 16: Normalized Flux for Alginate fouling conditions under a 1 kHz Field. Clean water (blue) lost 15% of flux during filtration. Alginate fouling with no field filtration (orange) lost up to 55% of flux. Continuous field application under Alginate fouling (grey) lost 13% of flux. Pulsed field application under alginate fouling (yellow) demonstrated similar performance to clean water filtration, losing 19% of flux throughout the trial.....	40
Figure 17: SEM image depicting top view and cross section of CTA membrane at 1mm resolution.....	46

Figure 18: SEM imaging of CTA membrane cross section at 100 micron resolution. The rejection layer can be seen on the bottom of the cross section as the smooth surface. Support and scaffolding layers are present as the mesh like material present above the smooth rejection layer.....	47
Figure 19: SEM image of membrane cross section at 50 micron resolution.....	48
Figure 20: SEM imaging of membrane cross section further zoomed in at 50 micron resolution. Greater detail is able to be seen in this image of both the rejection layer and support and scaffolding layer.....	49
Figure 21: FTIR analysis of bare CTA membrane.....	52
Figure 22: FTIR analysis of bare CTA membrane exposed to 1 kHz, 20 V AC electric field.....	53
Figure 23: FTIR analysis of CTA membrane fouled with BSA at 200 mg/L with 0.5 mM CaCl ₂	54
Figure 24: FTIR analysis of CTA membrane fouled with 200 mg/L BSA with 0.5 mM CaCl ₂ treated with a 1 kHz, 20 V AC electric field.....	55
Figure 25: FTIR analysis of CTA membrane fouled with 200 mg/L BSA with 0.5 mM CaCl ₂ treated with a 1 kHz, 20 V AC electric field.....	56

Chapter 1: Introduction

1.1 Problem Statement

Global water scarcity is one of the most critical issues that engineers and scientists face in the 21st century. Limited access to usable and potable water sources affects billions of people worldwide, leading to strain on the earth's existing water systems and causing massive displacement among populations [1]. As a result, there is a dire need to develop low-cost methods for producing usable water such as medical grade saline, particularly through the recycling and recovery of water from contaminated sources [2]. One such method for this extraction is forward osmosis (FO), a low energy membrane filtration process that relies on naturally occurring phenomenon to separate water from various solutions.

Forward osmosis is defined as the diffusion of water across a semi-permeable barrier due to the thermodynamic concentration gradient between two solutions; one of high solute concentration and one of low solute concentration [3]. In this diffusion, water will move from low solute (e.g., salt) concentration side to high concentration, bringing the system towards equilibrium. This water transport across the FO dilutes the solution of high solute concentration, and the system will move towards equilibria. As FO is driven by the concentration gradient, the applied transmembrane pressure (TMP) is not necessary. The lack of TMP requirement makes FO an economical and sustainable compared to reverse osmosis (RO), because less energy input means lower operational cost. Pressure ranges in RO vary from 125 to 1,200 psi, depending on the contaminant to be removed, which can lead to incredibly high operating costs [4]. FO was also shown to make up only 2-4% of the energy consumption of an FO-RO hybrid system, indicating that, when used in tandem,

the major energy requirement comes strictly from RO [5]. However, a direct cost analysis between FO and RO still needs to be done. FO membranes do not have pores, relying exclusively on diffusion and molecular transport for separation [6].

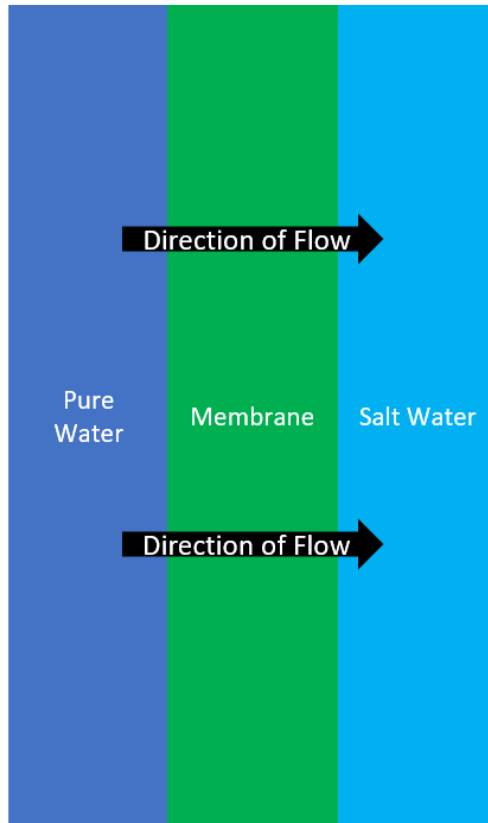


Figure 1: Schematic of Forward Osmosis principle. Water from the feed solution permeated into the draw solution across the concentration gradient, diluting the draw solution.

While FO is a highly promising alternative to future water treatment, there are still drawbacks to this process. The main drawback to FO is fouling in the long-term [6, 13, 16]. Foulants will slowly adsorb and adhere to the membrane surface, and then conglomerate and form layers on the membrane. This build up on the surface reduces the

transport pathways, and thereby reduces the water permeation rate through the membrane [6, 8, 13, 15, 16, 18].

In conventional membrane filtration, fouling occurs due to the contact between foulants and the membrane surface, as well as through compression onto the surface by the applied pressure. As foulants are pressed against the membrane surface, the adsorption and build-up of the foulant layer is accelerated. When the foulant layer completely blocks the transport of water, cleaning of the membrane is required. Membrane cleaning methods generally involve chemical cleaning and/or by flowing water at a high velocity across the surface, called shear flow cleaning, and flowing water across the membrane in the reverse direction, called backwashing [6, 7, 13].

The externally applied TMP is minimal in FO system. This leads to a much lower occurrence of fouling in the FO, as well as less compression of the foulant layer onto the membrane surface [8]. This in turn generally makes FO systems easier to clean through shear flow forces. The effect of fouling, however, is still prominent in FO and leads to significant flux decline, and therefore raises operating cost and increases downtime. There is a great need for development of a non-chemical based anti-fouling technique that can mitigate fouling while enhancing FO performance. FO is a highly promising technique especially for water recovery from wastewater streams because it has low propensity for fouling. [12]

Despite the advantages provided by FO, fouling is still a major concern that threatens to hamper the development of FO processes. A novel technique that uses of electric fields to remove fouling in-situ has shown to be promising [12]. In most applications, a direct current (DC) field is applied to induce electroosmosis, or the movement of charged

constituents within a bulk solution [14]. Limited research has been presented on the use of AC fields, however, since a paper in 1997 which presented the possibility for AC electric cleaning in ultrafiltration [15].

1.2 Summary of Research Contributions

The primary contribution this research will make in the field of membrane separation technologies stems from initially demonstrating the feasibility for AC fields as a viable method for FO fouling mitigation. Retaining high levels of flux over extended periods of operations is crucial for the advancement of membrane processes. This will increase both the usable lifetime of the membrane and productivity in the absence of blockage of water flow paths via fouling. The results from this research demonstrate the effectiveness of AC fields in mitigating fouling from model foulants, including bovine serum albumin (BSA) and sodium alginate (Alg), both in the presence and absence of a calcium chloride as the background electrolyte.

Experiments were conducted for three different electrical field settings: 10 kHz, 100 Hz, and 1 kHz in both continuous and pulsed AC fields. The permeate water flux in the presence of foulants were measured. Both membrane and foulant layers were characterized. For this research, a custom device FO system has been designed and fabricated. The main objective of this research is to establish a proof-of-concept for the feasibility of AC fields for mitigating organic fouling FO system. Based on the results thus far, several recommendations are included to help guide future experiments and improve upon these initial trials.

1.3 Thesis Outline

This thesis is organized into eight chapters. Chapter 2 is intended to serve as a thorough literature background exploring the current state of forward osmosis (FO) technology, an introduction to the fouling process in FO, the motivation for studying anti-fouling methods, and common measurement techniques for FO performance. Chapter 3 describes the testing methods used to quantify and monitor flux performance throughout separation trials. Chapter 4 is used to describe the foulants used in the study, as well as the composition of the feed and draw solutions used. Chapter 5 is a summary of the laboratory procedure and methods utilized in this research to explore flux performance under various conditions. Chapter 6 and Chapter 7 review the flux behavior under various foulant concentrations and electrical frequencies, and the membrane performance characterization under experimental conditions. Chapter 8 serves as a conclusion to this thesis with an overall summary of findings and recommendations. Chapter 9 contains a list of the references used in writing this thesis. Chapter 10 details the standard operating procedure and raw data used in the writing of this document.

Chapter 2: Literature Review

2.1 Forward Osmosis in Desalination and Fluid Recovery

Today, the increase in global water demand is driven by rising world population, climate change, expanding industry, and aging infrastructure [1, 16]. Due to depleting quality of freshwater resources around the world, areas with access to sea or brackish waters have started utilizing desalination as a means of meeting the region's water demand. The global water demand has been projected to exceed 36 billion cubic meters worldwide by 2025 [16, 17]. Desalination is a significant contributor to the overall water treatment and management market, being valued at \$12.8 billion USD in 2019, and is projected to continue to grow through 2027 [18]. Desalination techniques generally employ reverse osmosis (RO) for extracting potable water from saline sources, however RO desalination process is energy intensive and expensive to operate [17]. Furthermore, RO plants may have a negative impact upon the surrounding marine environment due to the discharge of highly concentrated brine that could disrupt entire ecosystems near the plant [19].

Forward osmosis (FO) has been investigated as an alternative method for desalination [5, 6, 13, 16, 17]. FO is a promising technique in the field of desalination since its driving force is the thermodynamic concentration gradient that exists between two solutions separated by a semipermeable barrier. Due to minimal pressure requirement, FO exhibits a lower propensity for fouling compared to RO, while maintaining a high salt rejection [16]. However, standalone FO systems are currently not developed enough to be used as a standalone desalination process. Some studies have shown FO to be more expensive in energy and operational cost due to the need to recover draw solutes to generate an end product [6, 16, 17]. FO does still have great contemporary promise as either an

auxiliary step or a pretreatment step in current RO plants, where the addition of the FO process has been shown to decrease the energy demand for the system by up to 1 kWh/m³ [5, 6, 17].

FO is also gaining traction and popularity in the general field of water reuse and fluid recovery. When used in tandem with membrane bioreactors (MBR), FO has been shown to be an effective method for the removal of organic matter from wastewaters in municipal and industrial treatment, and operates at a higher removal efficiency than traditional MBR [20, 21]. FO has been used to recover water from sewage [22]. FO has been explored for potable water production. For instance, NASA has tested a FO Bag which relies on glucose as a draw agent and urine as a feed solution for emergency water supplies aboard the international fire station (ISS) as recently as 2017. FO desalination plant in Oman has the treatment capacity up to 200 m³/day [21]. FO has been used in tandem with RO for the treatment of landfill leachate, wherein 80% - 90% of the contaminants removed and 90% of water recovered from the leachate [21]. Furthermore, other applications of FO include oil and gas, pharmaceutical, food and beverage industries among others [21]. FO is also currently being investigated for usage in the recovery of nuclear waste materials [23].

2.2 Fouling in Forward Osmosis Technologies

In pressure-driven membrane processes, a fluid is pressurized across a membrane to separate unwanted chemicals, particles, and/or solids from the product. These unwanted constituents may deposit and adhere to the membrane surface, potentially blocking the flow paths of water and thereby causes fouling [13].

One of the main advantages of FO as a fluid separation technology is the naturally occurring driving force from a concentration gradient. As mentioned previously, feed and draw solution are separated by a semipermeable barrier wherein the concentration gradient drives water to flow from feed side to draw side, and the second law of thermodynamics causes the system to work towards equilibrium. Thus, no transmembrane pressure is required for the FO operation. The lack of this applied pressure causes FO to have a lower propensity for fouling [6, 13, 16, 20].

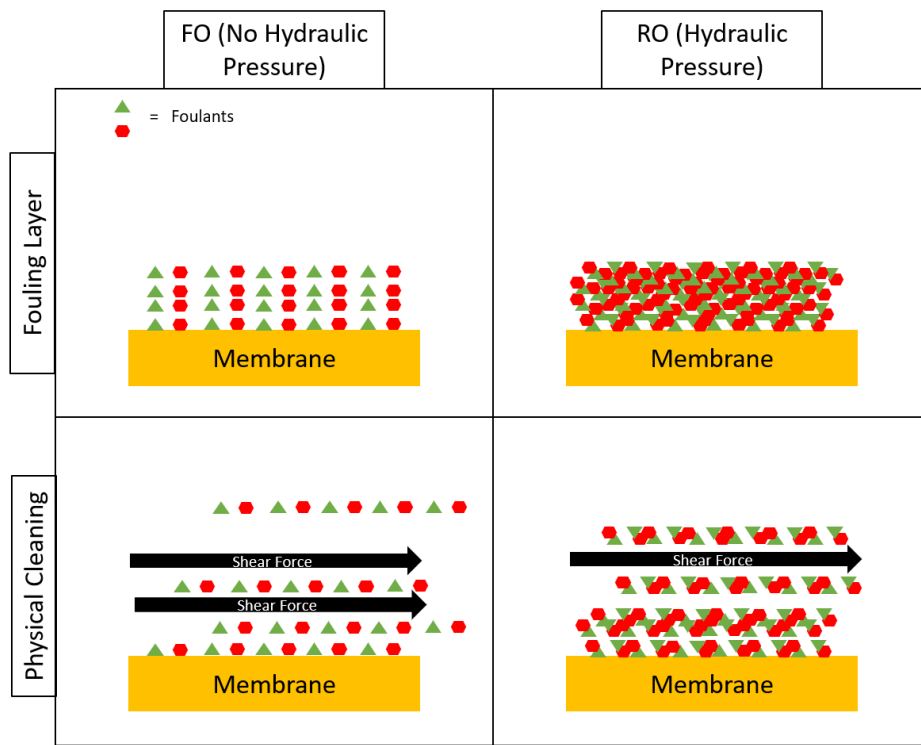


Figure 2: Comparison between fouling behaviors in reverse osmosis (RO) and forward osmosis (FO), demonstrating the effect of applied pressure on foulant layer. Higher applied pressures cause more severe fouling due to compaction of the fouling layer.

Fouling in FO generally occurs through three processes. First, hydrodynamic drag is generated by permeating water, pulling foulants within solution towards the membrane

surface. The resulting physical contact between the foulant and membrane surface can lead to adhesion or attachment of the foulant. Chemical interactions between the foulant, membrane, and other ions within the feed solution can further accelerate the fouling process by strengthening bonds between the foulant-foulant and foulant-membrane surface [6, 13, 24]. The build of foulants on the membrane surface leads to a dramatic decline in flux [25]. In addition, the membrane structure and properties can have a significant effect on flux performance. For instance, fouling propensity of a membrane increases with surface roughness [13]. The active layer of the membrane is smoother and does not have as many ridges or areas for the foulant to deposit, leading to a lower propensity for fouling through physical interactions [13]. The extent of fouling also depends on the surface charge of the membrane [20]. Absence of surface on membranes leads to minimal binding between the foulants and the surface [20]. Furthermore, hydrophobic membrane surfaces are prone greater fouling than the hydrophilic surfaces [20].

2.3 Anti-Fouling Methods and Practices in Forward Osmosis

2.3.1 Traditional Practices

Fouling poses one of the main threats to the advancement and implementation of membrane processes due to the drastic effect it has on flux performance and water recovery [6, 13, 16, 26]. A critical area of study within FO research has focused on methods for removing foulants from the membrane surface in order to extend membrane lifetime. Traditional membrane cleaning processes include physical and chemical cleaning methods [6, 13, 16].

There are a variety of physical membrane cleaning techniques. The most commonly used method is hydraulic flushing, where the crossflow velocity of the system is increased

to generate shear forces along the membrane surface and flush foulants out of the system [6, 7, 8, 13, 15, 16, 17, 23]. Osmotic backwashing, the process of reversing the concentrations of the feed and draw solutions to have water permeating in the opposite direction of operational permeation, has also been utilized as an effective method for the removal of colloidal particles trapped within the membrane structure [6, 7, 8, 13, 15, 16, 17, 23]. Sonic frequencies and the production of air bubbles near the membrane surface have also been explored as an in-situ method for the physical removal of foulants from the membrane surface [6, 15]. However, these methods are unable to remove all the foulants present on the membrane, and thus chemical methods are used for more severe fouling (i.e., irreversible fouling).

Chemical cleaning of membranes includes the use of acids, bases, and alcohols in order to scrub the membrane clean of specific foulants [6, 7, 8, 13, 15, 16, 17, 23]. Chemicals such as hydrochloric acid, citric acid and sodium hydroxide have all been utilized in various applications for the cleaning of membranes after fouling [6, 23]. While chemical cleaning is an effective method of foulant removal, there are several drawbacks that make it a non-ideal method. Constant exposure to harsh chemicals can cause damage to the membrane, rendering it unusable for future filtrations [15]. Furthermore, the replacement of the membranes along with the acquisition of these chemicals can increase the overall cost of the membrane processes. Recently, a few novel techniques including direct current (DC)- and alternating current (AC)-electric fields have been explored as an alternative method for the removal of foulants [REFs].

2.3.2 Electric Field Membrane Cleaning

The use of electric fields has been explored in filtration technologies to either improve the efficiency of the process or inhibit blocking of filtration paths since 1926 [15]. It was further built upon by researchers in 1967, who used electrical fields in tandem with ultrafiltration to separate clay suspensions in feedwater [27]. In electric field applications, membrane is sandwiched between two electrodes to allow the field to propagate across the surface [15]. When the electric field is turned on, the charged species in the solution migrate towards the electrode with opposite charge via a process called electrophoresis [15]. In addition, the electrical field can induce electroosmosis, wherein water flux and ionic species are mobilized in the direction of the field [28].

DC electric fields as an anti-fouling method have been explored to induce an electrophoretic effect on uniformly charged particles (foulants) [6]. Moulik et al., first observed this effect in their experiments with clay particles, noticing the clay being removed from the filter under the effect of the DC field [27]. Research in this field has focused mainly on the manipulation of membrane materials into an electrode [14, 29]. The effects of DC field on fouling mitigation have been shown to be effective with 90% of initial flux retention under fouling conditions using humic Acid [14]. However, the drawbacks [15] of DC fields include (1) electrolysis at the electrode surfaces, potentially producing lethal chlorine gas within the draw solution; (2) dramatic shifts in pH have also been observed under these operating conditions, which can damage the membrane surface and leave it impractical for further use; (3) corrosion of the electrode and high voltages can cause heating of the overall system as well as further damage to the membrane.

One application for electrical field membrane cleaning that is yet to be explored is the utilization of AC in lieu of DC. AC fields were first explored by Zumbusch et al., as an anti-fouling strategy during ultrafiltration of bovine serum albumin (BSA) as a model foulant [15]. Overall, a 40% improvement in flux retention was observed under a 25 Hz, 80 V/cm AC field under BSA fouling conditions, providing a strong indication that the fields were effective in reducing the occurrence of fouling in this experiment. However, since this publication, there is little to no further work conducted using AC as a means of in-situ electric field fouling mitigation. Due to newer methods of grafting and machining electrodes that can be thinner, and therefore experience smaller electrical resistance through the electrode, further exploring these effects will help to bridge the knowledge gap in the area of AC field-based antifouling mitigation methods.

2.4 Measuring Forward Osmosis Performance

The performance in FO systems is measured by quantifying the flux of the membrane, or the volume permeated per time per area of the membrane [23, 24, 30, 31]. In fouling experiments, permeate flux trend is used to study the effect of foulants on the FO performance. Flux decline is also a representation of the drop in osmotic pressure during FO operation.

$$\pi = iMRT \quad [1]$$

Where π is osmotic pressure, i is the van Hoff't constant, M is molar concentration, R is the universal gas constant, and T is temperature in Kelvin. Flux across the membrane is defined using the difference in osmotic pressure between the draw (π_d) and feed (π_f) solutions across the membrane area, as well as the water permeability, A [13].

$$J_w = A(\pi_d - \pi_f) \quad [2]$$

$$J_w = \frac{Volume}{Area*Time} \quad [3]$$

The volume of water collected is measured at specified intervals throughout the experiment duration. By plotting and examining the flux profile throughout the duration of the trial, it is possible to discern the percent retention of clean water flux obtained by the system during operation. This is referred to as normalized flux, and is represented by

$$J_N = \frac{J}{J_w} \quad [4]$$

Where J_N is referred to as normalized flux, the percentage of flux as a ratio to maximum flux, J is the flux obtained at any specific time point, and J_w is the clean water flux at time zero (maximum flux). By plotting the normalized flux versus time for each individual trial consisting of either no foulant in the feed, foulant solution as the feed, and foulant solution as the feed with electrical field, it is possible to draw conclusions regarding the electric fields ability to improve flux retention in the presence of foulant material.

Chapter 3. Testing Methods Employed in Research

3.1 Introduction

Flux is the most commonly used parameter to express the membrane performance in terms of permeation rate and water recovery. Measuring flux, the volumetric flow rate per unit membrane area, allows researchers to track and monitor the quantity of water being extracted from the feed solution during operation. Normalized flux (J_N) further enables researchers to compare different trials more accurately, particularly as the initial flux may vary with usages of different membrane coupons [20, 24, 26, 31]. Traditionally, fouling experiments are performed under various conditions of the feed solution to quantify the effects of different foulants on membrane performance through flux. For this research, fouling experiments were performed with and without foulant solution to gauge the effect on fouling in traditional FO experiments. Fouling experiments were then replicated using the foulant solution and AC electric fields. These trials were compared in order to gauge the effect of the AC electric field FO flux.

Clean water flux (J_w), the flux loss in the presence of feed solution with no foulants, enables the quantification of flux decline as water permeates from the feed into the draw solution, and thereby the natural loss of osmotic pressure across the membrane. As water permeates through the membrane from the feed solution containing foulants into the draw solution, the concentration of the salt in draw solution decreases, and the concentration of contaminants in feed increases. Comparing these clean water and fouling trials allows for the quantification of flux loss during FO process [20, 24, 26, 31].

Experiments with and without foulants in the presence and absence of AC fields were conducted to evaluate the effect of the electric field on fouling in FO. Fouling was

studied in the presence of a low-frequency, low-voltage oscillating electric field to gain mechanistic insights into foulant-membrane interactions. In these experiments, the AC electric field is simply turned on and studied fouling under two different modes: 1) continuous field and (2) pulsed field for the entire duration of the trial. In the pulsed field mode, the field was turned on only for a brief period at specified timepoints throughout the trial, following the procedure reported in Zumbusch et al. [15, 32]. These experiments were performed in order to gauge any effect the electric field would have on the fouling behavior in terms of flux performance.

3.2 Testing Device

This research employed traditional FO flux procedures employed by a variety of researchers [5, 6, 7, 8, 10, 12-14, 16, 17, 19, 22-26, 29-31, 37]. Typically, a crossflow filtration unit is used consisting of two halves of a module: one for the feed and the other for the draw solution. A membrane is sandwiched between the two halves, and the module is then sealed. The feed and draw solutions are pumped into their respective parts of the FO filtration cell under crossflow conditions. The concentration gradient between the two feeds across the membranes causes water to permeate into the draw solution. The membrane material used in this research consisted of a cellulose triacetate (CTA) polymer provided by FTSH₂O, formerly HTI (Albany, Oregon). These membranes are widely used in the field of FO science due to their low fouling propensity and high chlorine tolerance of up to 2 parts per million in wide pH range of 3-7 [33, 34].

Many companies sell commercial FO modules for use in the lab setting [34], but at this stage they have not been developed to apply electric fields. Consequently, we have fabricated a custom-made filtration module that can apply electric fields on demand during

the FO process. The cell was fabricated out of Delrin plastic, or polyoxymethylene, a material that is chemically resistant with a high stiffness. The cell was made with a filtration channel consisting of 7 cm × 17.5 cm × 1 cm on either side of the module, with inlet and outlet ports lining either side of the feed and draw modules. This cell consisted of two separate O-ring channels used to create a seal within the filtration channel and prevent leakage. Prior to each test, the cell was calibrated using mass balance approach to ensure volume lost by feed solution is gained by draw solution. The cell also was tested for leaks at various times throughout each trial, ensuring a closed loop within both feed and draw solution.

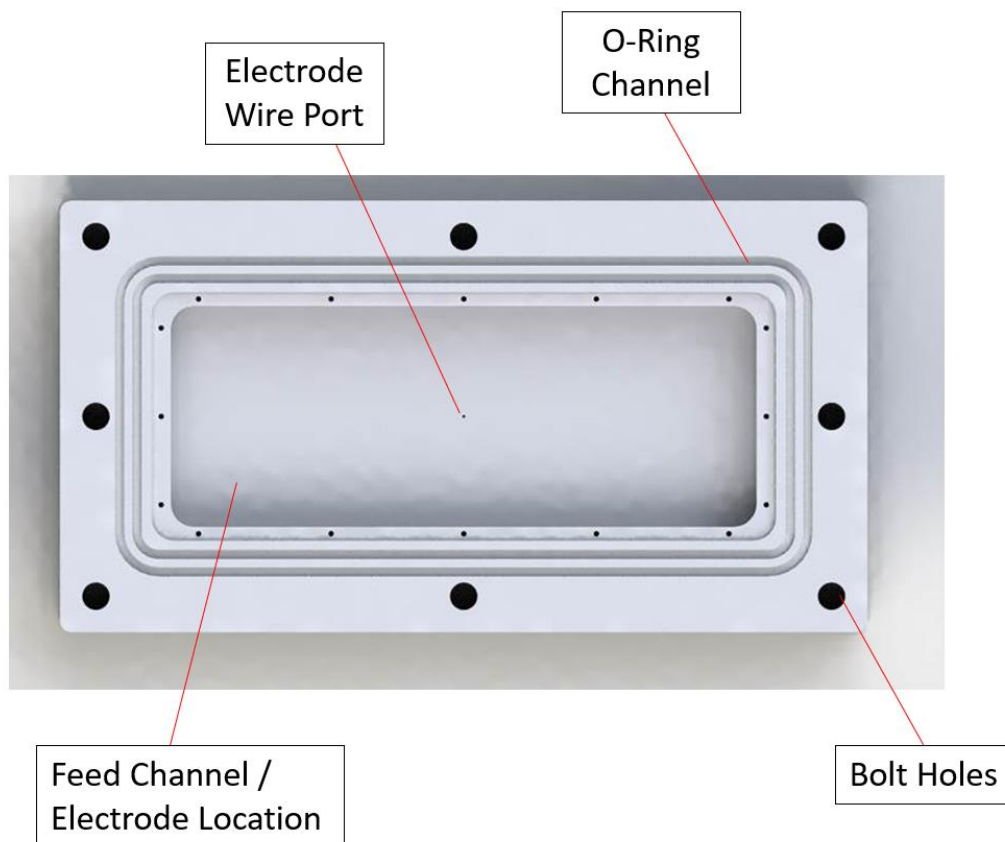


Figure 3. Top view of filtration cell produced for use in this study.



Figure 4: Side view of filtration cell produced for study, showing location of inlet and outlet ports.

To propagate the electric field across the membrane, a small hole was drilled into the surface of either cell to allow a 24-gauge platinum wire to pass through into the filtration channel. These wires were then attached to a carbon paper electrode procured from the fuel cell store (Sigracet 29 BC, Fuel Cell Store, Bryan, Texas), and oriented so that the direction of the electric field was always perpendicular to the membrane surface. The wires were connected to a function generator (Siglent, SDG1025, Solon, Ohio) and an oscilloscope (Tektronix, TDS2012, Beaverton, Oregon) used to apply and control the electric field, respectively.

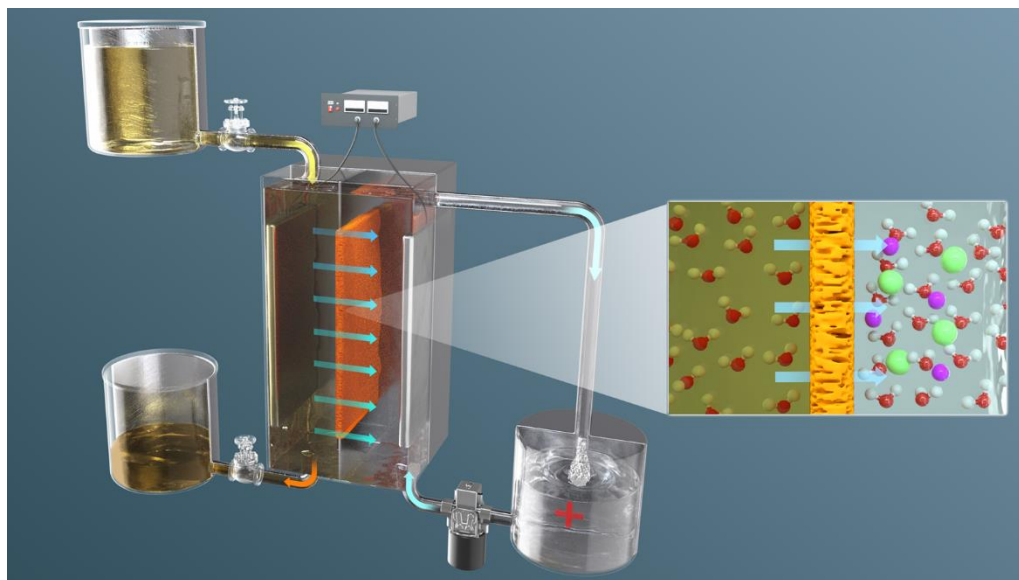


Figure 5. Schematic drawing of experimental set up. Feed solution (left) provides water to permeate into the draw solution (right). A power supply is hooked up to the electrodes, and the electric field is applied in the direction of permeating water, perpendicular to the membrane surface.

The feed and draw solutions resided in separate Nalgene containers (volume), and Ismatec ISM184 eight-channel pumps heads (Cole-Palmer) were used to create flow in both feed and draw solution channels. The draw solution tank was placed on an OHAUS AX8201/E Adventurer scale connected to a computer, where water weight readings were recorded every 15 seconds. The weight measurements were then converted to volume for flux calculations. Future research possibilities based on the improvement of this device are included in Chapter 8.

Chapter 4: Foulants, Feed and Draw Solution Composition, and Membrane Material

4.1 Introduction

The model foulants used in this study were bovine serum albumin (BSA) and sodium alginate. They were employed in two different types of solution with calcium chloride as an electrolyte to accelerate chemical bonding between foulant-foulant and foulant-membrane. Tests were also conducted without an electrolyte to examine hydrodynamically driven fouling. Both BSA and sodium alginate are model protein and polysaccharide, respectively, foulants commonly used to model organic fouling and biofouling in FO [5, 6, 7, 8, 10, 12-14, 16, 17, 19, 22-26, 29-31, 37]. The fouling from BSA and alginate were studied in the presence and absence of electric fields in order to determine the critical fields at which fouling could be mitigated.

4.2 Bovine Serum Albumin

BSA is a hydrophobic globular protein used in various industrial processes including vaccine production, food and pet food manufacturing, and drug delivery applications as well as protein studies [36]. BSA is a commonly used model foulant in a variety of membrane studies, generally used to represent proteins in water and wastewaters [37]. Proteins in general make up a large fraction of nitrogen and carbon present in wastewater effluents and influents, are generally present in many environments abundant with vertebrae and other organisms [38, 39]. Furthermore, proteins are a major constituent of organic matter in wastewater influents and effluents, making proteins such as BSA a favorable choice for representation of organic matter in membrane processes [25, 40]. BSA

has a molecular weight of around 66 kilodaltons, and is generally found in a pH range of 5.2 – 7 [41].

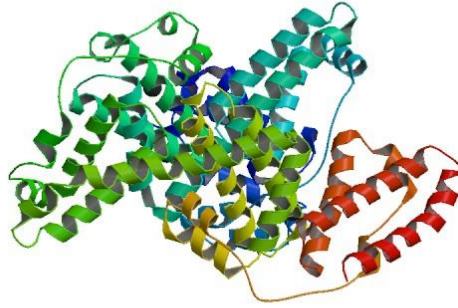


Figure 6. Representation of the BSA molecule, obtained from the Royal Protein Database [42].

Several studies have suggested BSA fouling is mostly dominated by hydrodynamic forces near the membrane surface [24, 25, 37]. In the presence of an electrolyte (e.g., 0.5 mM CaCl₂), no major change in the loss of flux was observed in FO experiments conducted by Mi et al., [24]. Instead, BSA fouling is mostly driven by adsorption or attachment to the membrane surface, followed by further interactions between the BSA molecules. Furthermore, adhesion forces measured through atomic force microscopy by Mi et al., indicated similar levels of adhesion between BSA and the membrane surface with and without the presence of an electrolyte. This was attributed to the relatively low presence of carboxylic groups in BSA, which would allow for a reduced level of chemical complexes to form between BSA and the membrane.

4.3 Sodium Alginate

Sodium alginate is a naturally occurring polysaccharide commonly derived from brown algae and seaweeds. It is widely used in the food and pharmaceutical manufacturing

process due to its ability to retain water and form a gel in aqueous solutions [43]. As a naturally occurring substance in many natural waters, alginate is widely used as a model foulant to represent natural organic matter [25]. It is abundantly present in wastewaters and identified as one of the major organic foulants of concern in various membrane operating facilities [44]. Sodium alginate has a molecular weight of 216.12 g/mol and is highly soluble in water [45].

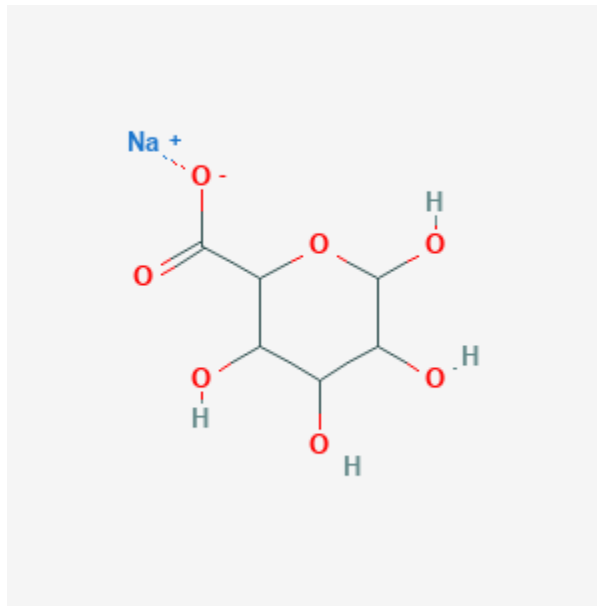


Figure 7. Chemical structure of the sodium alginate molecule, obtained from the National Library of Medicine [45].

As a foulant, hydroxyl groups on sodium alginate will form chemical bonds with the carboxylic groups on the membrane surface via cations present in the background electrolyte in a process called chemical bridging [13, 24, 25]. As a result, alginate fouling tends to be very severe, but can be removed through periodic cleaning using physical methods [44]. When severely fouled, alginate forms a dense gel layer that causes dramatic flux decline in FO [24, 25, 41, 44].

4.4 Feed Solutions

In a FO process, first, feed solution typically with low solute concentration is exposed to a draw solution with high solute concentration through a cellulose triacetate (CTA) membrane. The concentration gradients between the solutions drives water from feed to draw solution causing feed to lose volume while draw to gain weight. Foulants in the feed gradually accumulate and adhere to the membrane surface resulting in fouling.

Feed solutions used in this research were chosen based on similar feed solutions used in previously published research [24, 26, 31, 44]. The feed solution used for clean water experiments consisted of strictly ultrapure water. For initial fouling experiments, 1 g/L BSA was used as a feed solution to study severity of fouling in the presence and absence of electric fields. In addition, experiments in the absence of electrolyte were also conducted to study effect of electric fields on BSA fouling due to hydrodynamic drag forces. Similar to BSA experiments, alginate fouling tests with and without electric fields were also conducted. The feed solution consisted of 200 mg/L sodium alginate with and without 0.5 mM CaCl_2 as background electrolyte. Lastly, experiments were also conducted using 200 mg/L BSA with 0.5 mM CaCl_2 as the background electrolyte to further investigate a potential difference in the ability of the electric field to mitigate fouling in the presence of chemically accelerated fouling. The composition of feed solutions used in different test are summarized in Table 1.

Table 1: Summary of composition of feed solutions used in this research.

Test	Concentration
Clean Water	Ultrapure water No foulant present
BSA Fouling	Ultrapure water 1 g/L BSA
BSA Fouling with CaCl ₂	Ultrapure Water 200 mg/L BSA 0.5 mM CaCl ₂
Alginate Fouling with CaCl ₂	Ultrapure Water 200 mg/L Alginate 0.5 mM CaCl ₂

4.5 Draw Solution

The draw solution is the concentrated salt solution used to generate the concentration gradient against feed solution to generate forward osmosis. In this study, a 1 M sodium chloride solution was used as the draw solution to generate a concentration gradient. After the first set of trials using this draw solution were concluded, it was decided to replace this solution with a 1.5 M NaCl solution for the draw in order to generate higher values of initial flux, and higher rates of initial fouling. Furthermore, this concentration was chosen to represent twice the salt content of seawater, which is generally estimated to be 0.7 M NaCl.

4.6 Cellulose Triacetate Membrane

The FO membrane material used in this study made of the polymer cellulose triacetate (CTA) with an embedded polyester mesh for mechanical strength. CTA was first synthesized and commercialized by Hydration Technologies Inc. now FTSH₂O (Albany, OR), in 2006 as a low fouling membrane material [46]. CTA membranes are classified and defined per US patent US7445712B2 as an asymmetric membrane comprising of a skin layer made of a polymeric material serving as a rejection surface, a porous layer of the same material as the rejection surface serving as a scaffold for the rejection layer, and a hydrophilic support fabric [46]. The thickness of CTA membranes is approximately 50 μm [6-8, 10, 12-14, 16, 17, 19, 22-26, 29, 30, 31, 37].

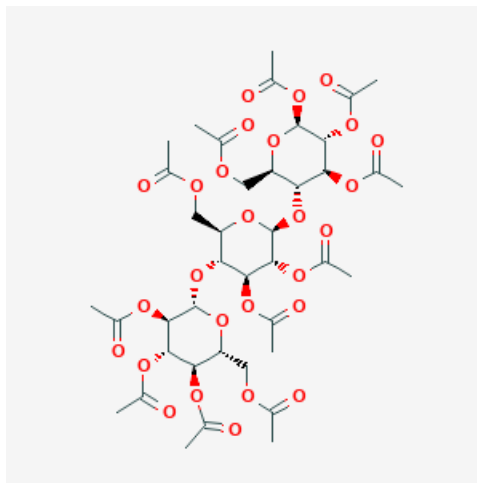


Figure 8: Chemical structure of cellulose triacetate, obtained from the National Library of Medicine [61].

Chapter 5: Laboratory Methods to Induce Fouling

5.1 Introduction

The method used to induce membrane fouling by BSA and sodium alginate on the cellulose triacetate (CTA) membrane is described in this section. For all of the FO processes with and without foulants, the fouling is to occur for an 8-hour period both in the presence and absence of electric fields. The FO fouling was studied at three different frequencies including 100 Hz, 1 kHz, and 10 kHz at 20 V_{p-p} [Chapter 6]. The membranes were then examined using a surface electron microscopy (SEM) and through atomic force microscopy (AFM) [Chapter 7]. In addition, foulants on the membrane surface were analyzed using Fourier transform infrared (FTIR) spectroscopy for changes in composition [Chapter 7].

5.2 Method Explored

In this research, the FO experiments were performed with a bench-scale set up depicted in Figure 9.



Figure 9. Lab scale set up utilized for this research. Draw solution (left) is placed on a scale to monitor changes in volume. Feed solution (right) is continuously stirred to ensure the solution is well mixed.

The following steps were implemented for each experiment. First, the CTA membrane was placed within the filtration unit with the active layer facing the feed solution. Next, 1 L of ultrapure water (resistivity 18 MOhm) and 500 mL of ultrapure water were added to the draw and feed tanks, both placed on a digital scale, respectively. The pumps were used to pump the liquids in a closed loop, going from the solution tanks, through the two-channeled membrane unit, and back to the tanks, for 8 hours to ensure proper hydration of the membrane, remove any air bubbles from either closed loop, and allow for stabilization of flows within the filtration system. At this point, stock solution of 3 M NaCl was added to the draw solution tank in proper quantities to bring the NaCl concentration of the draw solution to 1.5 M. At this point, the data collection program was started to record weight changes by a computer in real time to determine permeate water

flux. In the clean water flux trials, FO experiments were conducted using 1 M NaCl for 1 hour to determine the maximum initial flux as well as stabilized flux after osmotic dilution. In fouling experiments, stock solution of foulant solution was added into the feed solution to reach pre-determined concentrations (1 g/L BSA and 200 mg/L sodium alginate), and the FO process was carried out for a period of 6-8 hours. Temperature was monitored using a handheld probe at the beginning and conclusion of each trial to ensure temperature remained constant during the experiment.

All of the FO fouling experiments in the presence of electric fields were conducted following the steps described above. For these trials, the platinum wires were connected to the feed and draw solution channels of the FO cell via alligator clips to the function generator. The platinum wires attached to the electrodes were sealed in the feed and draw solution cells using a chemically and thermally inert epoxy glue. The electric field trials were conducted in two modes: constant field and pulsed field. Constant field trials were conducted by turning on the function generator output immediately after mixing the foulant stock solution with the feed solution, and the field was kept on for the duration of the trial. Pulsed field experiments were performed by turning on the function generator for 2-minute intervals spaced between 2-hour intervals of no field. This process repeated until the conclusion of the filtration trial. The FO performance in the presence of foulants and electric fields were evaluated. Specifically, the effect electric field frequencies 100 Hz, 1 kHz and 10 kHz at constant strength 10 V/cm on BSA and alginate was investigated.

The field was also monitored going into the cell by using a voltmeter on the draw and feed solution wires connecting into the cell to ensure proper conduction into the flow channels. Each electrode was also tested during the conduction of each trial to ensure the

field was being propagated. In the event an electrode did not register on the voltmeter, it was removed, the area where it was occupied was cleaned with an ethanol rinse and replaced with a new electrode. If an electrode ceased to register on the voltmeter during an electric field trial, the experiment was stopped, and the electrode replaced.

Baseline experiments, denoted as clean water flux trials, were also performed in order to gauge flux decline based purely on osmotic dilutions. These trials followed the same protocol as described above, with no fouling solution added to the feed stock. The fouling trials were conducted immediately after clean water trials in order to ensure similar performance of the cell was achieved. The cell was cleaned using a 70% ethanol solution in between each trial and rinsed with ultrapure and deionized water to ensure no outside contamination was present. All tests were performed in triplicate. The normalized flux data versus time were plotted to examine the behavior of flux throughout the duration of each experiment.

5.3 Advantages and Limitations of the Method Explored

The expansion of this research using different types of membrane materials, such as, would help to improve the understanding of the effect of electric fields on a broad range of materials, as well as help to improve this area of study in general. Furthermore, the results from a crossflow flat sheet FO membrane module may differ from results obtained from a different membrane module, such as a spiral wound or hollow fiber membrane set up. Further research in this area using various membrane modules and materials would greatly benefit the overall knowledge in this field.

An additional set back that must be acknowledged is the shutdown of the University sponsored lab in which this research was conducted during COVID-19. The original intent

of this research was to also include foulants such as bacteria and viruses in the study for a more complete view of biofouling behavior in the presence of AC electric fields. The shutdown limited the time allowed in the lab, and this additional research was unable to be obtained. For this reason, several trials including BSA with CaCl_2 were performed as single experiments instead of triplicates.

Chapter 6: Antifouling Experiments with Electric Field

6.1 Introduction

Methods to explore flux performance in the presence of foulant material were utilized in order to compare obtained results to similar tests in published literature. The tests performed FO experiments with no foulants present, BSA at 1 g/L and no electrolyte as a foulant, alginate at 200 mg/L with 0.5 mM CaCl_2 as a background electrolyte, and BSA at 200 mg/L with 0.5 mM CaCl_2 as a background electrolyte. These tests were then repeated in the presence of a 100 Hz, 1 kHz, and 10 kHz electric field at a voltage of 20 volts AC in both a continuous and pulsed setting as described in Chapter 5. All tests were performed in triplicate, with the exception of some BSA in combination with CaCl_2 tests, which were performed in single trials due to time constraints associated with COVID-19. All filtration trials were averaged and plotted versus time to examine the behavior of flux throughout the duration of each experiment. All testing procedures used are described in Chapter 5 of this document.

6.2 Results and Discussion

6.2.1 BSA Fouling in Absence of Electrolyte

Initially, several trials were conducted in order to calibrate the FO cell used in this research. After confirming the integrity of the device, triplicate experiments were

performed to yield an average normalized flux drop across each set of trials. The clean water flux profile served as a baseline for comparison with conditions under fouling. In total, triplicate experiments were conducted for BSA fouling under (1) no field, (2) a constant oscillating field, and (3) a pulsed oscillating field applied for 2-minute intervals after 2 hours of no field. These trials were all conducted using a 1 kHz, 20 V_{p-p} electric field to establish an initial proof-of-concept for this research. Figure 10 below demonstrates flux behavior obtained in each of these trials.

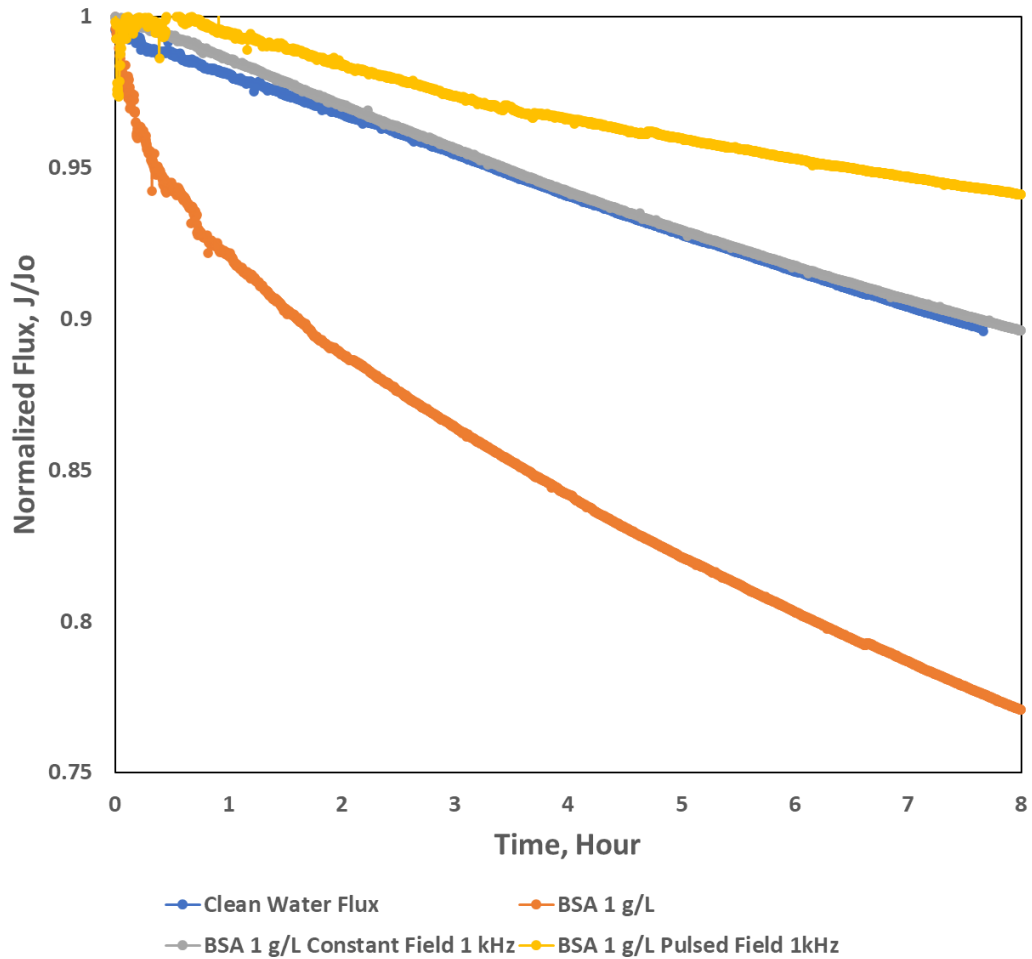


Figure 10: Normalized flux for BSA fouling conditions for 1 g/L concentration and no CaCl₂ with 1 kHz 20 V_{p-p} electric field. Clean water (blue) experienced a 10% loss in initial flux. BSA fouling with no field (orange) lost 25% of flux performance over the course of the filtration. Continuous field (yellow) application in fouling conditions decreased the percentage of flux lost, with a 10% of flux loss over the duration of the trial. Pulsed field (grey) in fouling condition trials saw an improvement of flux performance compared to clean water, losing only 5% of flux over 8 hours.

In the absence of foulants, an overall 10% clean water flux loss due to osmotic dilution of 1.5 M NaCl? draw solution was observed at the end of 8 h. This flux loss is due to the loss of concentration gradient as water molecules permeate across the membrane surface from the feed solution. In the presence of BSA with no electric field, 22.5%

cumulative flux loss was observed at the end of 8 h. In the presence of BSA and constant electric field, set to 1 kHz frequency and 20 V AC, the flux loss was only 10%, which is similar to the clean water flux loss. In the presence of BSA and pulsed fields (1 kHz frequency and 20 V AC), the overall flux loss was only 5%, which is lower than the clean water flux. This result suggests that water recovery is significantly higher than both clean water flux and BSA with constant field. Overall, both trials conducted in the presence of an electric field and BSA at 1 g/L as a foulant demonstrated an increased flux retention when compared to traditional BSA fouling conditions.

6.2.2 BSA Fouling in Presence of Calcium Chloride Electrolyte

Following the conclusion of experiments using 1 g/L BSA with no electrolytes present, it was determined prudent to also include an examination of BSA at 200 mg/L with 0.5 mM calcium chloride present. This decision was made in order to accelerate BSA fouling via chemical bridging of BSA-BSA and BSA-membrane via calcium ions. These tests took place after the reopening of the lab post COVID-19 related shutdowns within the University. All tests were conducted in triplicate. Data from some of the trials had to be discarded due to various errors that occurred with the FO cell operation. Mainly, blockage within the draw and feed solution loops was found within the pressure regulators which would build up throughout the duration of fouling trials, causing erratic and unreliable flux behavior and data collection. These tests were all discarded, and a full cleaning of both feed and draw loops was implemented using a 50% ethanol solution over a 24-hour period. After several tests to ensure proper performance of the FO cell were carried out, data collection resumed. However, this unexpected delay caused several problems in data collection. Mainly, the timeframe in which this additional research was to be conducted

closed, and each test was only able to be performed with a single replicate, which created difficulty in drawing concrete conclusions from the data. Furthermore, only constant field trials were able to be performed in this setting, preventing any conclusions from being drawn with this fouling solution in tandem with the pulsed field application. The constant field trials are presented in their singular results compared to the data obtained from fouling of BSA at 200 mg/L with 0.5mM calcium chloride as well as the corresponding clean water flux yielded from the baseline experiments in each trial in Figures 11-13.

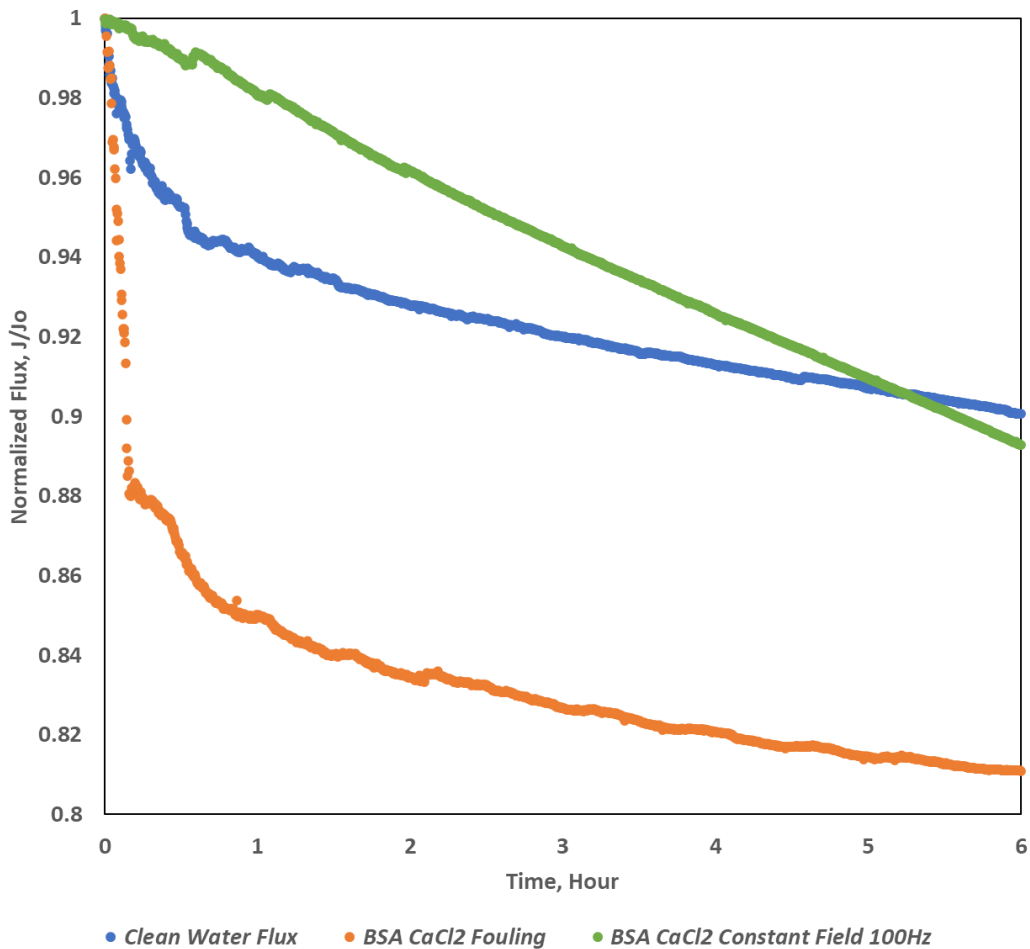


Figure 11: Normalized flux for BSA fouling conditions for 200 mg/L concentration and 0.5 mM CaCl₂ at 100 Hz 20 V_{p-p} electric field. Clean water (blue) experienced a 10% loss in initial flux. BSA fouling with no field (orange) lost 19% of flux performance over the course of the filtration. Continuous field

(green) application in fouling conditions decreased the percentage of flux lost, with a 11% of flux loss over the duration of the trial.

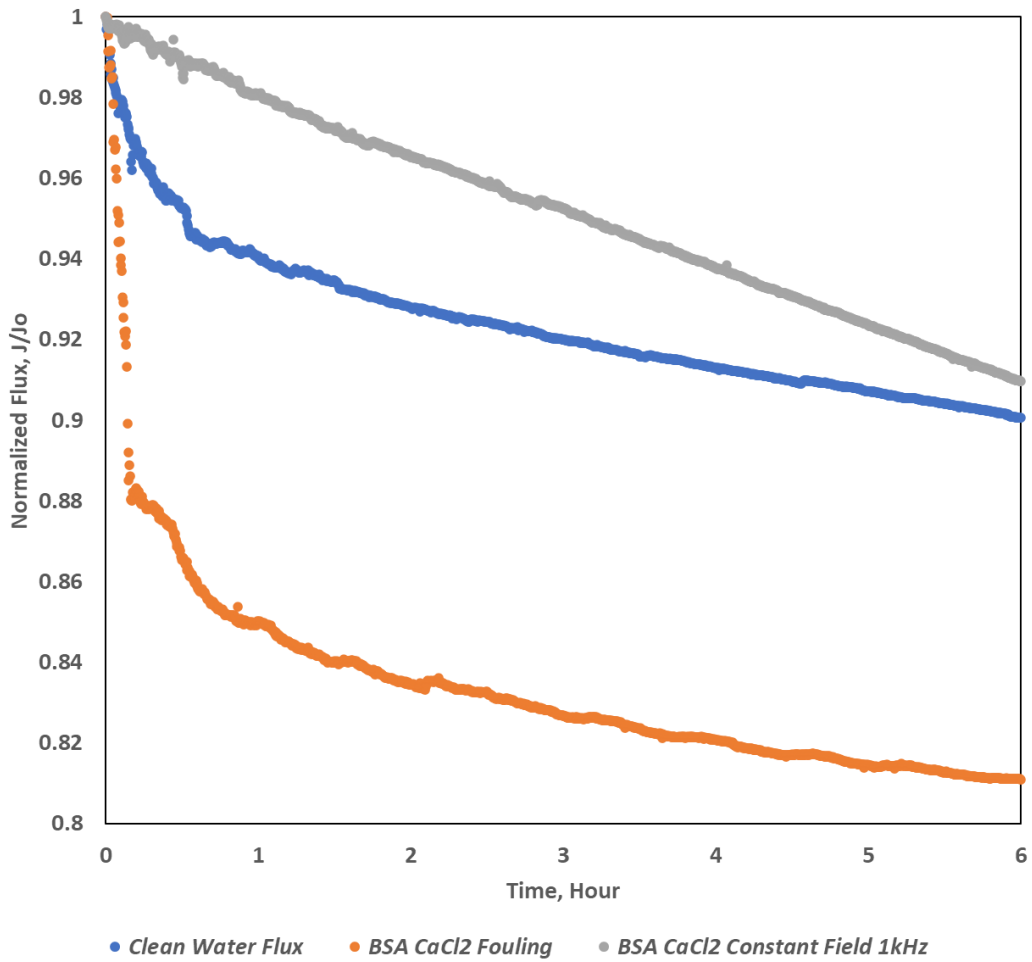


Figure 12: Normalized flux for BSA fouling conditions for 200 mg/L concentration and 0.5 mM CaCl₂ at 1 kHz 20 V_{p-p} electric field. Clean water (blue) experienced a 10% loss in initial flux. BSA fouling with no field (orange) lost 19% of flux performance over the course of the filtration. Continuous field (grey) application in fouling conditions decreased the percentage of flux lost, with a 9% of flux loss over the duration of the trial.

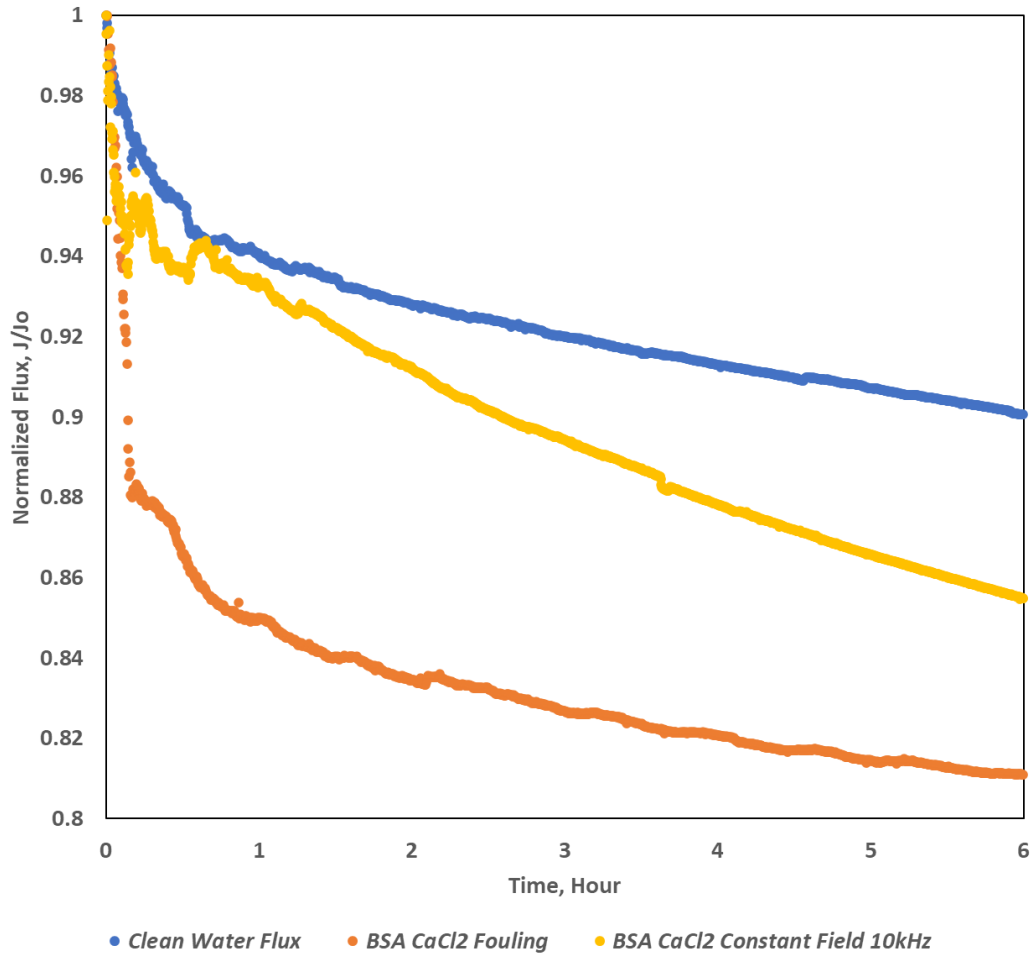


Figure 13: Normalized flux for BSA fouling conditions for 200 mg/L concentration and 0.5 mM CaCl₂ at 100 Hz 20 V_{p-p} electric field. Clean water (blue) experienced a 10% loss in initial flux. BSA fouling with no field (orange) lost 19% of flux performance over the course of the filtration. Continuous field (yellow) application in fouling conditions decreased the percentage of flux lost, with a 15% of flux loss over the duration of the trial.

Based on data obtained from these trials (Figures 11-13), clean water flux using a 1.5 M sodium chloride solution exhibited flux loss of 10% on average over 6 hours due to osmotic dilution of the draw solution. In terms of BSA fouling at a concentration of 200 mg/L with 0.5 mM calcium chloride present, flux loss was similar to the case using 1 g/L and no CaCl₂, with a flux decline of 19% vs. 22.5% on average. These findings are

consistent with the results published by Mi *et al.*, which observed the difference in fouling behavior of BSA at 200 mg/L both with and without the presence of CaCl₂ [24]. This is attributed to BSA fouling being dominated by hydrodynamic forces, and limited chemical interactions between the BSA and membrane surface.

Data from the single constant field trials once again yielded improved flux decline compared to the BSA fouling with no field present, which is also similar to clean water flux. Under a 100 Hz field, an overall flux loss was observed to be 11% under the single trial conducted. Flux loss under 200 mg/L BSA with 0.5 mM CaCl₂ in the presence of a 1 kHz field demonstrated a 9% loss in flux in the single trial performed. Lastly, flux behavior in experiments using BSA at 200 mg/L and 0.5 mM CaCl₂ in tandem with a 10 kHz constant field presented a flux decline of 15% after the conclusion of the FO trials.

6.2.3 Alginate Fouling

Experiments were conducted to study alginate fouling in the presence of an AC electric field using 200 mg/L sodium alginate with 0.5 mM calcium chloride, referred to in this section as the alginate solution. These experiments were performed following the initial calibration of the filtration cell and proof-of-concept BSA data. All trials were performed in triplicates, and the average normalized flux decline was used for analysis. All values obtained for normalized flux for each experimental condition are presented in Figures 14-16.

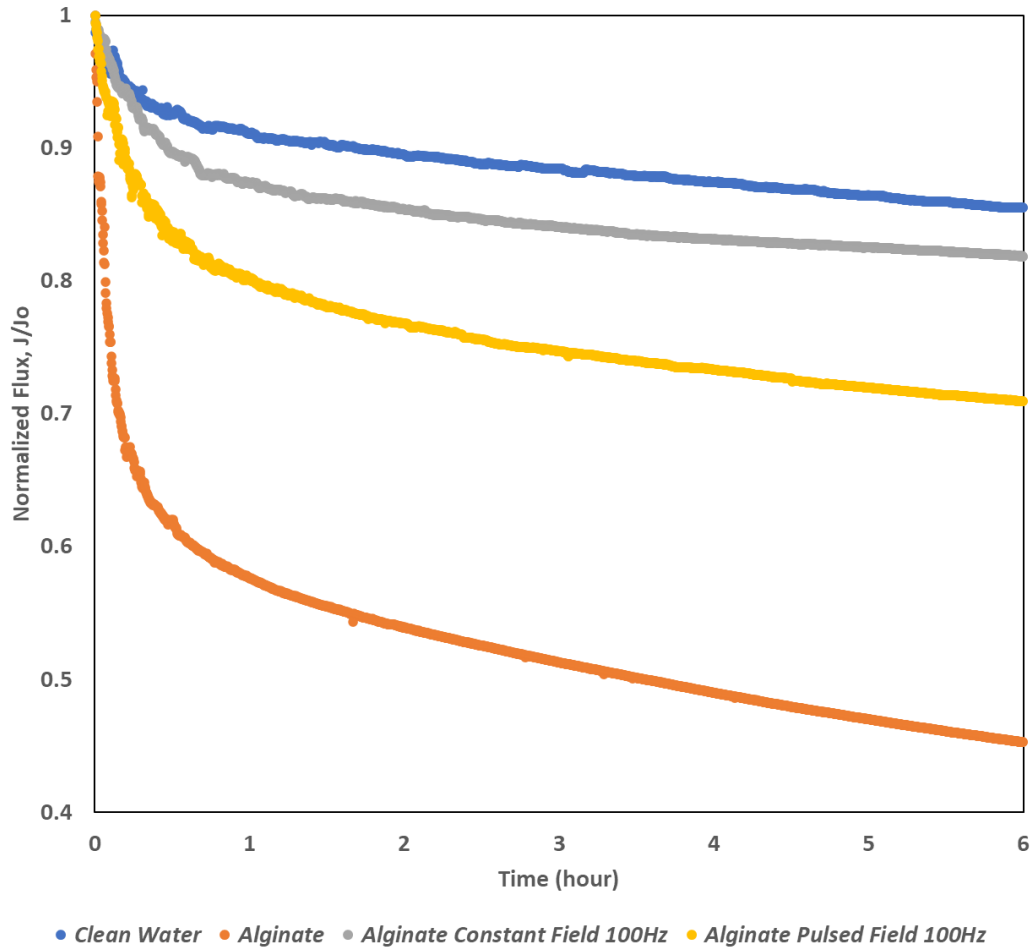


Figure 14: Normalized Flux for Alginate fouling conditions under a 100 Hz Field. Clean water (blue) lost 15% of flux during filtration. Alginate fouling with no field filtration (orange) lost up to 55% of flux. Continuous field application under Alginate fouling (grey) lost 19% of flux. Pulsed field application under alginate fouling (yellow) demonstrated similar performance to clean water filtration, losing 30% of flux throughout the trial. Insert Alginate and CaCl₂ concentration.

Results obtained from alginate fouling trials under 100 Hz electric field conditions are shown in Figure 14. Clean water flux values presented in this graph are a representation of an average of all clean water baseline trials conducted prior to alginate fouling trials. On average, osmotic dilution of the draw solution during these trials accounted for 15% of initial flux loss. FO fouling due to alginate trials were performed in triplicate. The results

showed a flux decline of 55% to 45% of initial flux at the conclusion of the trial. This decline was attributed to alginate fouling. The 100 Hz constant field improved flux retention in the presence of alginate fouling when all trials were averaged together. The flux retention was improved by 20% with 100 Hz constant field flux during alginate fouling. The 100 Hz pulsed field application improved flux retention when compared to traditional alginate fouling, with flux declining by 30% of initial flux across an average of all trials conducted, as compared to the 55% to 45% observed in the control group (normal fouling conditions). In both cases, with 100 Hz electric field, an improvement in membrane flux retention was observed.

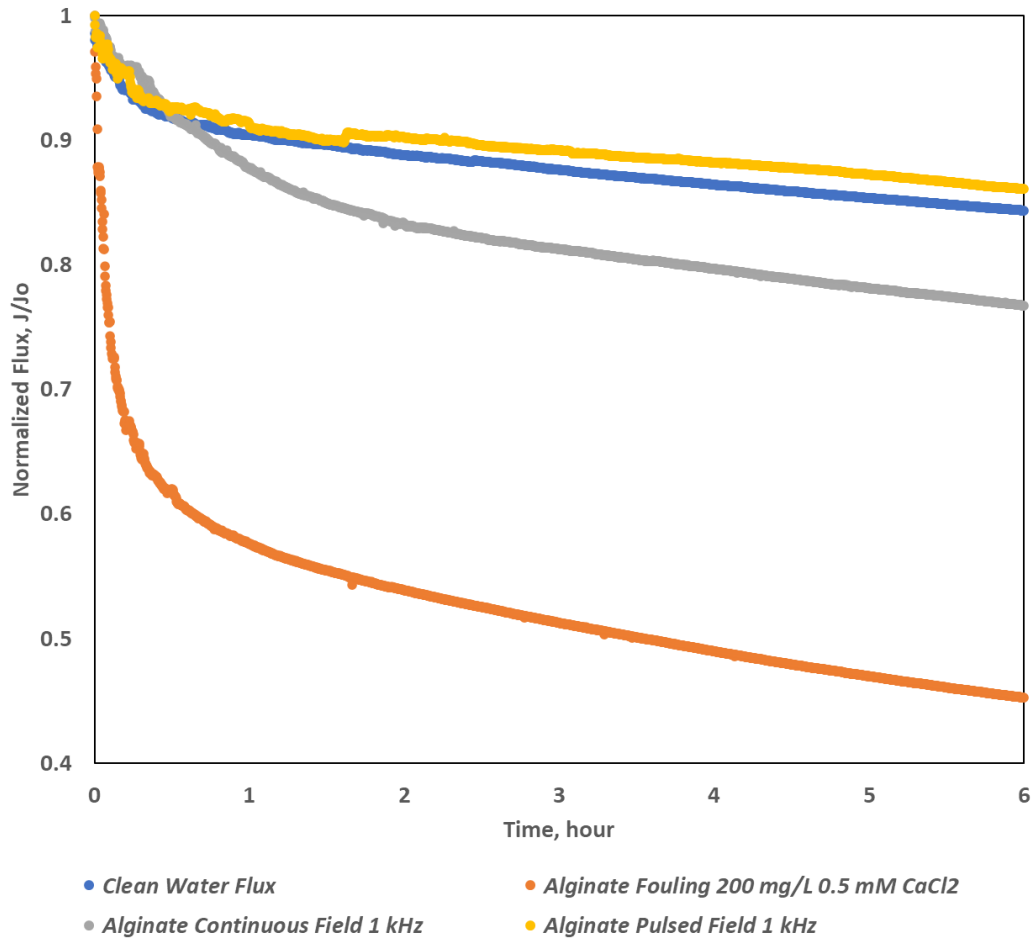


Figure 15: Normalized Flux for Alginate fouling conditions under a 1 kHz Field. Clean water (blue) lost 15% of flux during filtration. Alginate fouling with no field filtration (orange) lost up to 55% of flux. Continuous field application under Alginate fouling (grey) lost 24% of flux. Pulsed field application under alginate fouling (yellow) demonstrated similar performance to clean water filtration, losing 14% of flux throughout the trial.

Experiments conducted using a 1 kHz electric field are shown in Figure 15. Clean water and alginate fouling experiments are the same as shown in Figure 14, as both are derived from an average of all trials conducted with the alginate fouling solution. Flux decline for clean water and alginate fouling with no field in these settings was observed to be 15% and 55%, respectively. In the 1 kHz setting, the constant field experiments showed a flux

decline of 24% of initial flux on average. Pulsed field trials using 1 kHz AC field showed a flux decline of 14% of initial flux when averaged across all trials.

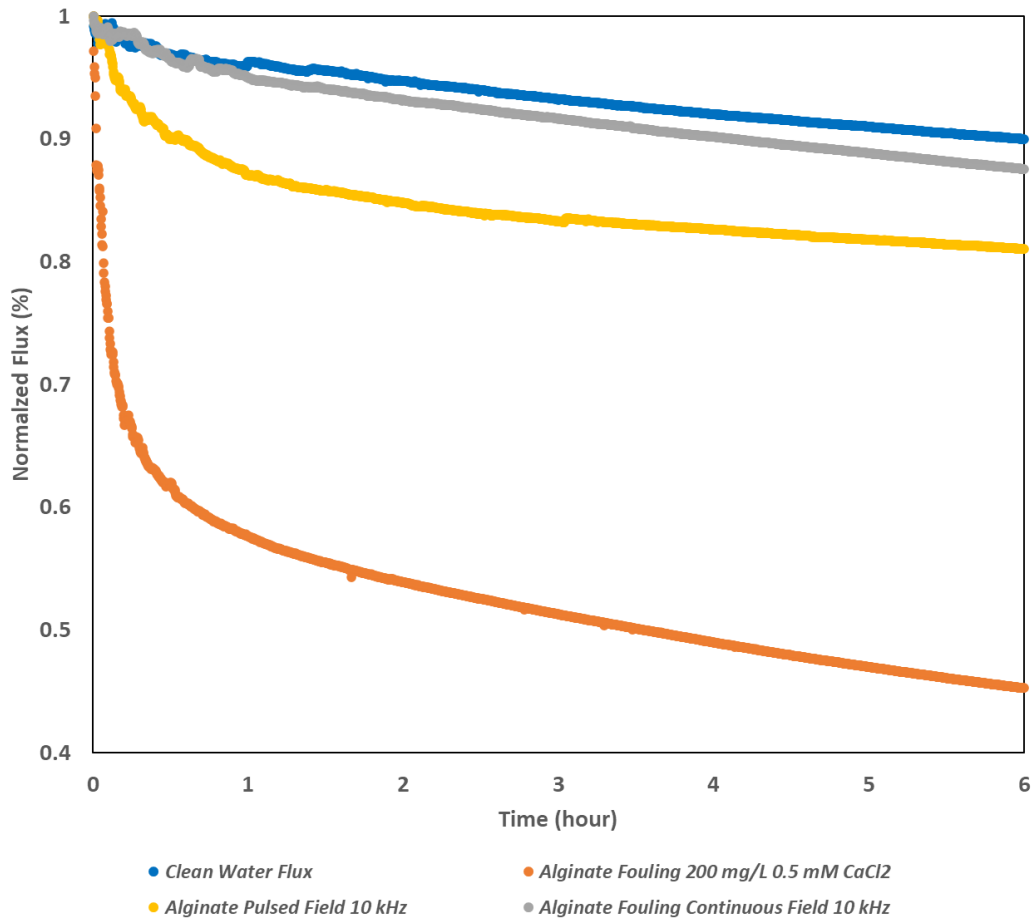


Figure 16: Normalized Flux for Alginate fouling conditions under a 1 kHz Field. Clean water (blue) lost 15% of flux during filtration. Alginate fouling with no field filtration (orange) lost up to 55% of flux. Continuous field application under Alginate fouling (grey) lost 13% of flux. Pulsed field application under alginate fouling (yellow) demonstrated similar performance to clean water filtration, losing 19% of flux throughout the trial.

Experiments using 10 kHz electric field are shown in Figure 16. Prior to conducting these trials, an extensive clean of the operating system was performed due to construction that had occurred in the lab prior to the start of these experiments. To ensure there was no

debris within either loop of the membrane, a 50% ethanol solution was passed through each loop at a pressure of 10 psi for a period of 48 hours. A new tubing material was also used at the inlet and outlet of the pump used to generate flow through the feed solution, as the previously used material experienced several ruptures at the onset of these trials. Therefore, a different set of clean water experiments was presented in these trials in order to more accurately compare the clean water baseline experiments to the field experiments. Alginate fouling trials shown in these trials remain the same as presented in Figures 14 and 15.

The results showed that clean water flux decline due to osmotic dilution was observed to account for a 10% loss of initial flux. Alginate fouling resulted in a 55% loss of initial flux. Constant field trials conducted using the 10 kHz field demonstrate a loss of flux of 13% across an average of all three replicates. Pulsed field experiments at frequency of 10 kHz exhibited a flux loss of 19% on average after conclusion of filtration trials.

6.3 Conclusions

Across all trials performed, flux loss observed during the baseline clean water experiments was found to range from 10% - 15%. This flux loss due to osmotic dilution is unavoidable in experiments where the draw solution is not continuously replenished and follows a similar trend to published results using similar draw solutions [24, 44]. At 1 g/L, BSA fouling was observed to cause flux to decline by 22.5% over the duration of the trial, compared to 19% when the solution composition was changed to 200 mg/L with 0.5 mM calcium chloride. It should be noted that the 200 mg/L BSA with CaCl₂ trials were only conducted in duplicate, however both flux decline values are comparable and similar to published literature using BSA [24]. Alginate fouling was observed to cause flux to decline by 55% when used at a concentration of 200 mg/L with 0.5 mM calcium chloride present

as a background electrolyte. This obtained value is also comparable to similar studies on the behavior of alginate fouling [24, 31].

Experiments with the electrical field overall demonstrate an improvement in flux retention in the presence of fouling material across all trials performed. Electrical fields at 1 kHz and 20 Volts peak to peak used in tandem with 1 g/L BSA solution cause a decrease in flux loss, or an increase in flux retention, from 22.5% up to 10% and 5%, respectively. In both cases, flux retention is improved to values similar to clean water flux, or flux behavior as if there was no foulant present in the feed solution. An increase in flux retention was observed in the presence of 200 mg/L BSA solution with 0.5 mM calcium chloride in tandem with the field across all trials. In experiments conducted using 100 Hz 20 V electric field, a constant field flux loss values decreased from 19% to 11%. Compared to the clean water flux loss of 10%, it is once again observed that the electric field improved flux retention under fouling conditions. Under 1 kHz constant field, it is observed that flux retention improved from 19% under fouling conditions to 9%, once again demonstrating performance similar to clean water trials. The 10 kHz constant field was also found to improve flux retention, with a 15% loss of flux being observed in the presence of the field versus 19% with no field present.

Fouling experiments using sodium alginate with calcium chloride present as a background electrolyte further demonstrate the effect of an electric field to improve flux retention, or decrease the magnitude of flux decline, across all trials performed. In these trials, alginate fouling was found to reduce flux by 55% on average. Starting with 100 Hz experiments under alginate fouling conditions, it can be observed that both constant field and pulsed field applications improved the flux performance, with flux loss values of 19%

and 30%, respectively. Flux performance under 1 kHz frequency electric fields also demonstrated an increased retention of flux, with constant and pulsed electric field applications improving flux loss from 55% to 24% and 14%, respectively. 10 kHz trials also followed this trend, with flux loss values decreasing from 55% to 13% and 19% under a constant and pulsed field application, respectively.

Across all trials, the data demonstrates that an AC field application increased the retention of flux under fouling conditions. In general, under 100 Hz and 10 kHz applications, the constant field application resulted in a higher magnitude of flux retention. Under the 1 kHz application, in both BSA and alginate conditions, it can be observed that not only was the pulsed field application more effective in terms of flux performance under fouling conditions, but also demonstrated improved performance compared to clean water trials. This could be explained several ways. First, it can be observed that the actual variation in values of flux retention between pulsed and clean water applications are minimal, and therefore are insignificant when compared. A second explanation could be found by investigation of the hydrodynamic conditions near the membrane surface under application of the field. Increased turbulence of the feed and draw solution near the membrane surface caused by oscillations induced by the electric field could increase mixing and reduce the degree of concentration polarization. Concentration polarization occurs in the osmotic process as water permeates across the membrane. The water molecules build up at the boundary layer of the membrane on the draw side, decreasing the concentration at the boundary layer. Conversely, on the feed solution boundary layer, the concentration is at a higher concentration than the bulk solution due to constant dehydration and permeation of water molecules [47]. This phenomenon contributes to a significant

amount of flux decline in FO, however, was not the main topic of this study. The investigation of any effects an AC electric field may have on concentration polarization is an area of further research that should be investigated. A comprehensive suggestion of future research in this direction is included in Chapter 8.

Chapter 7: Membrane Characterization

7.1 Introduction

Common methods for the characterization of the bare membrane and membrane with fouling material was performed as part of this research. These methods include SEM imaging, AFM imaging, and Raman Spectroscopy. Several replicates of each type of material were provided. Only SEM images of the bare membrane were able to be obtained, as the procedure for examining the CTA membrane under SEM required dehydration by freeze drying in liquid nitrogen. This caused any fouling material on the membrane to be removed. However, a cross section of the CTA membrane is still beneficial for the purpose of background and explanation of fouling occurrence. AFM images were obtained of the foulants on the membrane. Due to a major backlog in the AFM lab caused by COVID-19, some samples were unable to be sampled multiple times. In the AFM imaging obtained of the fouled membranes with foulant present, no image was able to be obtained by the microscope, and as a result these images were not included in this report. Raman Spectroscopy results were affected by a similar backlog and unavailability of the lab post COVID-19 shutdown, however a full array of BSA fouling data (clean water, BSA fouling, BSA fouling under 1 kHz field) was able to be obtained for this study.

7.2 SEM Imaging

Surface electron microscopy (SEM) is a method of imaging involving beaming a concentrated electrons onto a surface, exciting the atoms on the surface [48]. The microscope then registers and receives a signal based on the reaction of the atoms on the surface being studied and is able to produce a high-resolution image. SEM is widely used in membrane studies to examine and characterize the membrane surface [24, 49]. All

images were obtained through the University of Vermont Health Science Research Facility.

SEM images obtained for this study are presented in Figures 17-20 below.

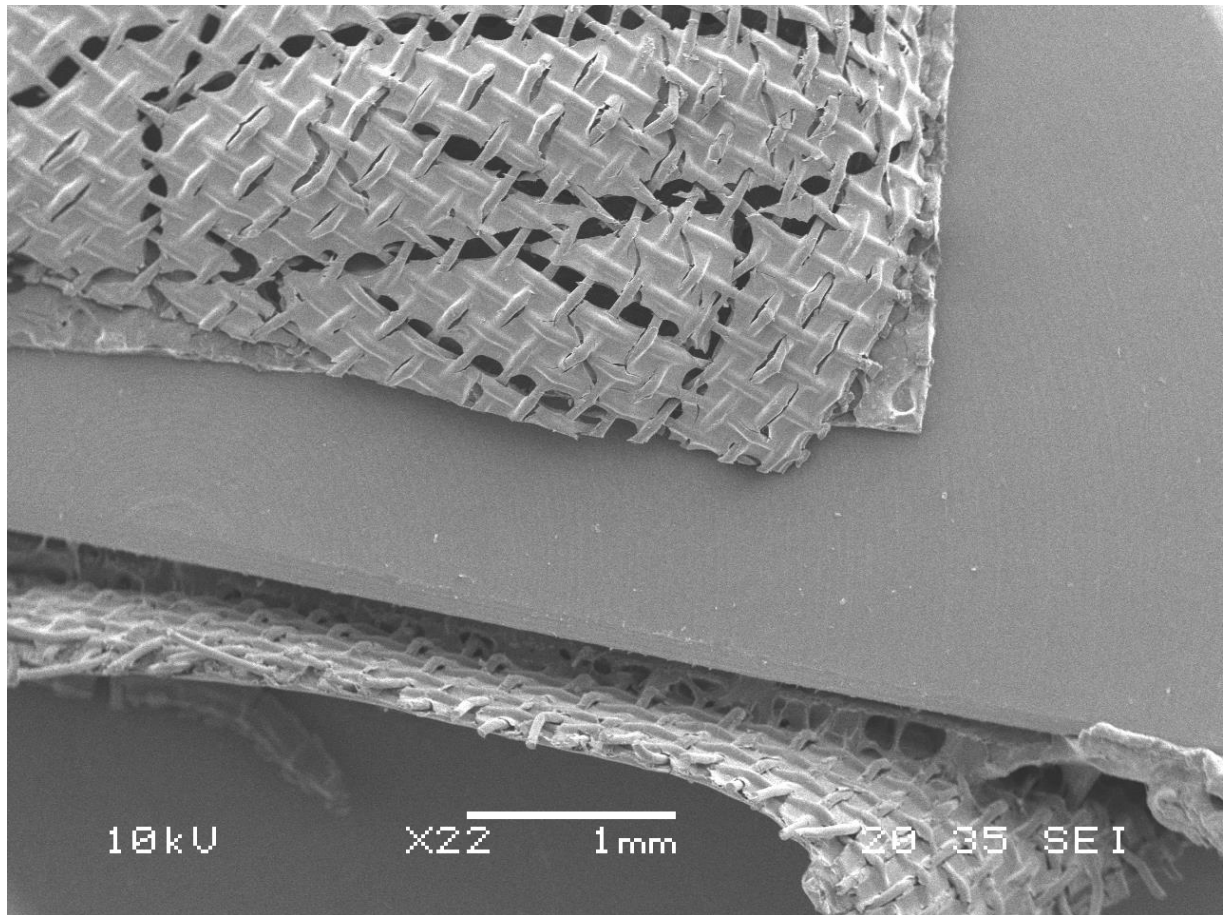


Figure 17: SEM image depicting top view and cross section of CTA membrane at 1mm resolution.

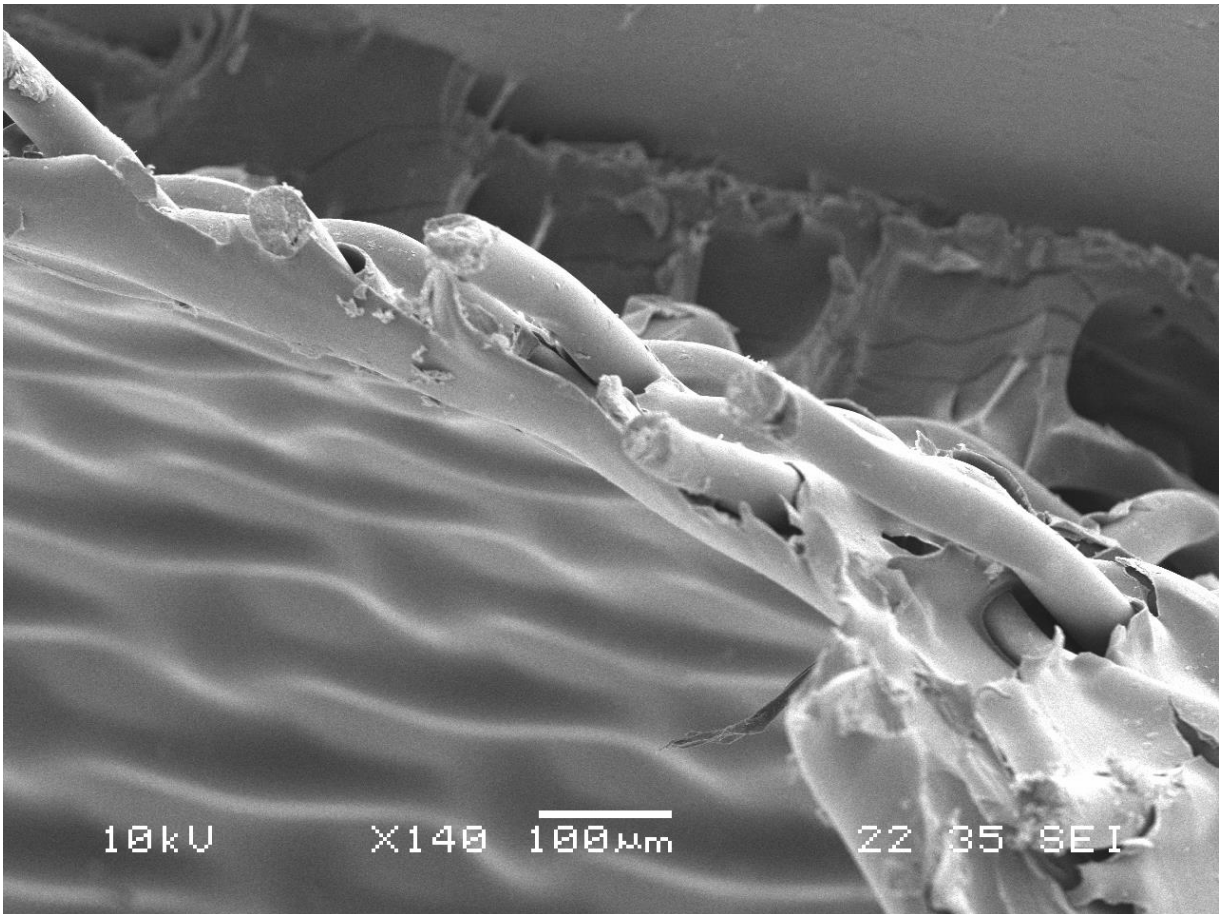


Figure 18: SEM imaging of CTA membrane cross section at 100-micron resolution. The rejection layer can be seen on the bottom of the cross section as the smooth surface. Support and scaffolding layers are present as the mesh like material present above the smooth rejection layer.

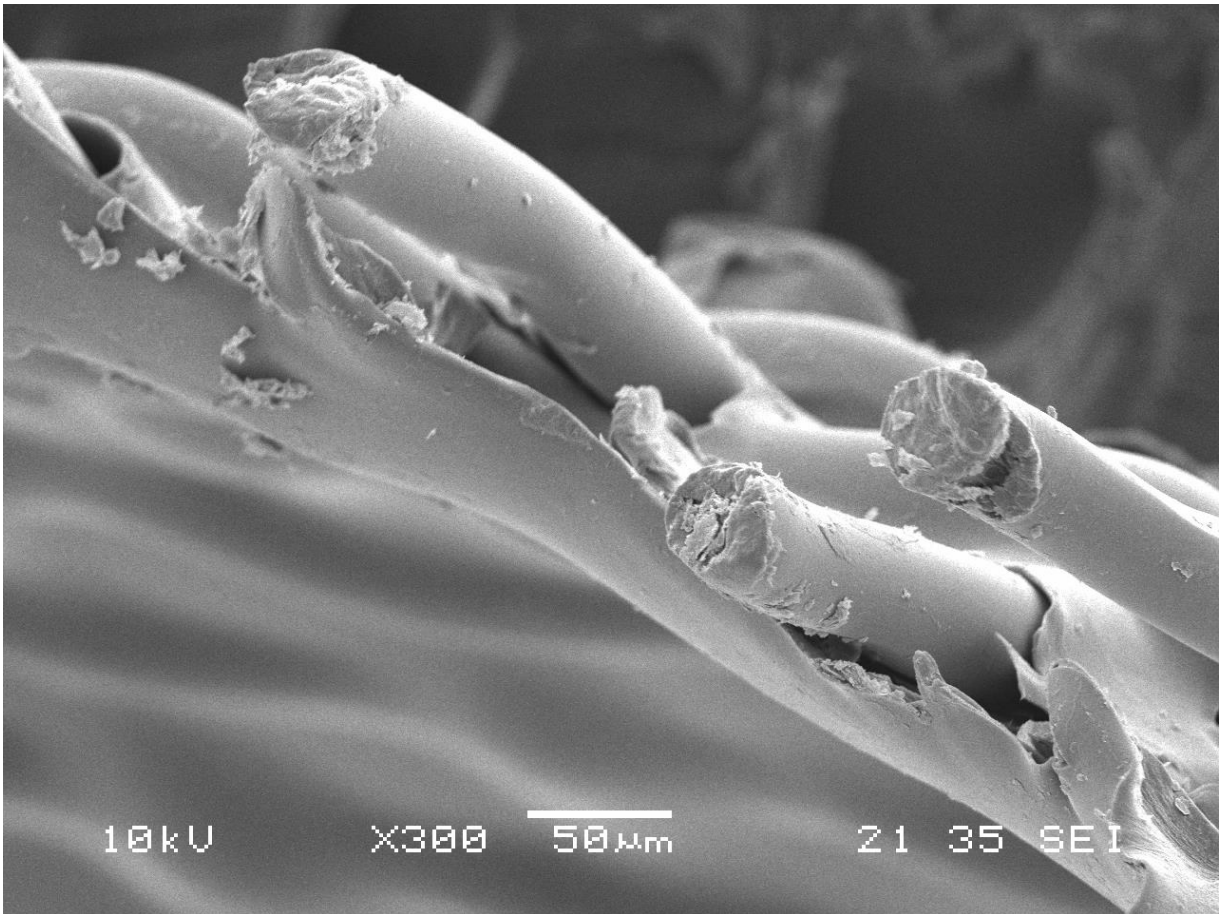


Figure 19: SEM image of membrane cross section at 50-micron resolution.

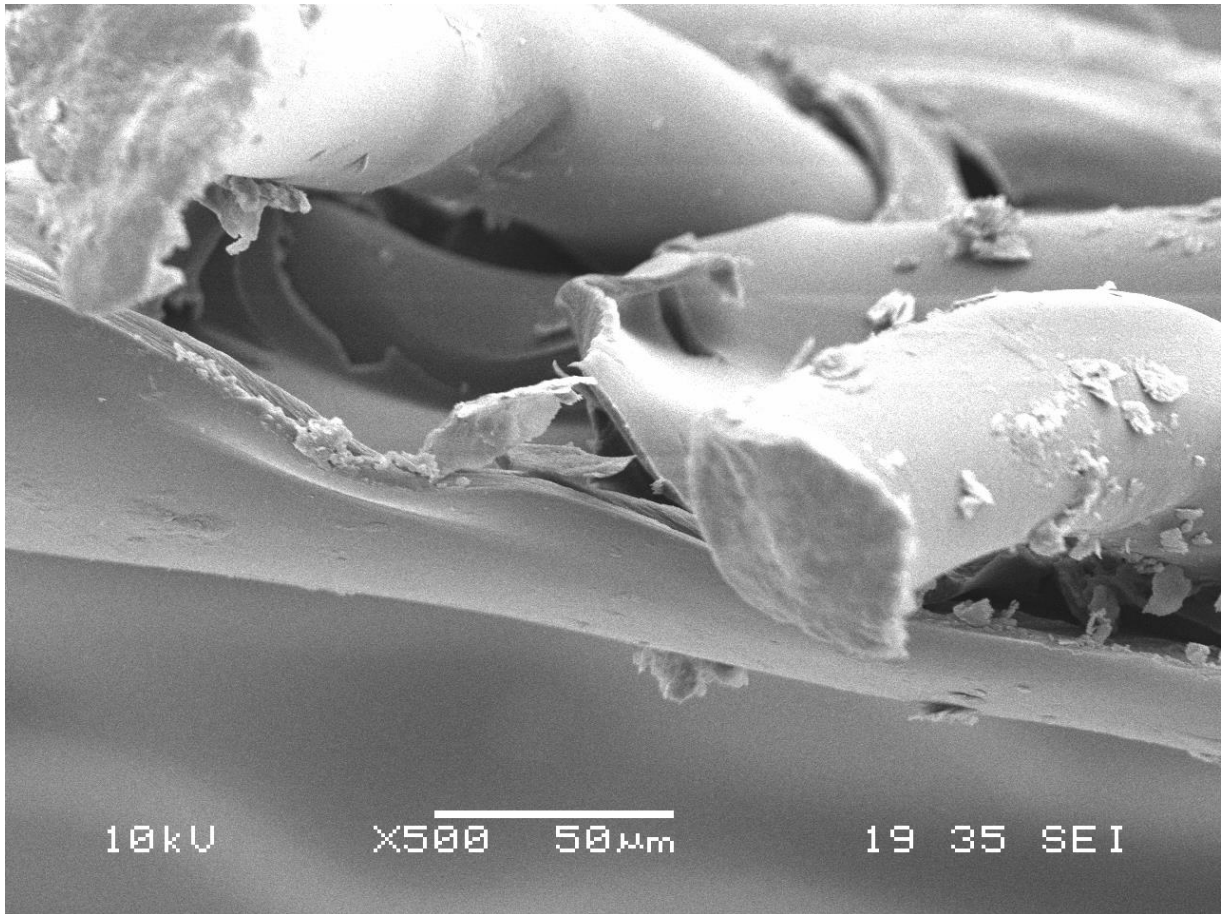


Figure 20: SEM imaging of membrane cross section further zoomed in at 50-micron resolution. Greater detail is able to be seen in this image of both the rejection layer and support and scaffolding layer.

Figure 17 depict a top view and cross-sectional view of the SEM membrane. As described in Chapter 4.6, CTA membranes are characterized as an asymmetric membrane comprising of a polymeric rejection layer supported by a porous scaffold layer made from the same polymeric material. The rejection layer serves to reject all molecules but water or solvent from permeating across the membrane, while the support layer serves as structural support. Figure 18 shows the top view of the rejection layer, with the porous support layer visible as the mesh-like material underneath, as well as the cross-sectional view. Figures

19-20 provide higher resolution images of the cross section of the membrane, with the rejection and support layers becoming clearly visible.

7.3 AFM Imaging

Atomic Force Microscopy (AFM) is a probing imaging tool that operates by running a small (3-6 micrometer) tip with a 15-40 nanometer radius tip over an object [50]. As the probe is run over a sample, a cantilever moves the probe according to changes in height detected on the surface. This results in a topographical image of the sample. AFM can also be used to measure adhesion forces between objects and is greatly useful in the area of membrane science for measuring adhesion between foulants and membrane material [24]. All AFM analysis performed for this study was conducted at the University of Vermont Health Science Research Facility. Samples tested for this study include bare CTA, CTA fouled with BSA, CTA fouled with alginate, and both fouled membranes in the presence of the field. Unfortunately, no conclusions can be drawn from the AFM analysis. In the case of the BSA fouled samples, the CTA fouled with BSA without the field sample was unable to be registered by the AFM microscope, and so a comparison between the BSA fouled membrane with and without the field by AFM was not able to be performed. For the alginate fouled membrane, both samples were unable to be detected by the probe, so no data was able to be collected. Therefore, all AFM images collected were not included in this study as no reasonable conclusions were able to be drawn from them.

7.4 Fourier Transform Infrared (FTIR) Spectroscopy

FTIR operates by passing infrared light through a sample to a detector. The sample will absorb some of the light passing through, allowing the rest of the light to pass to the detector. Individual compounds will absorb a specific amount of this light, which can be

used to identify species in a solution [51]. FTIR was used to ensure that there are no electrolysis products forming at the electrodes in the draw or feed solution, as well as to monitor any other biproducts that form during the application of the electric field. FTIR analysis was only able to be performed on a bare CTA membrane, a CTA membrane exposed to the field to detect any potential changes to the membrane surface itself by exposure to the electric field, a CTA membrane fouled with BSA, and a CTA membrane fouled with BSA exposed to a 1 kHz electric field. Alginate fouled samples were not able to be tested due to a severe backlog of samples to be analyzed after the University shutdown due to COVID-19. All analysis was performed by the University of Vermont Department of Chemistry. Figures 21-25 depict analysis yielded by FTIR analysis of these samples.

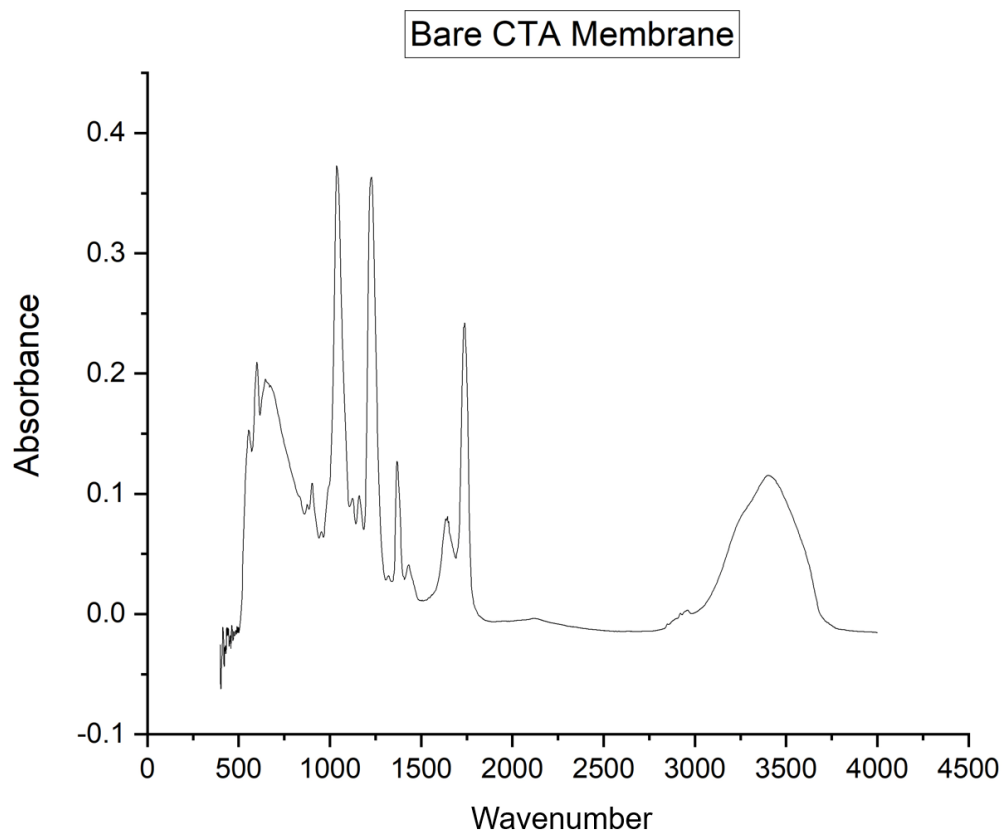


Figure 21: FTIR analysis of bare CTA membrane.

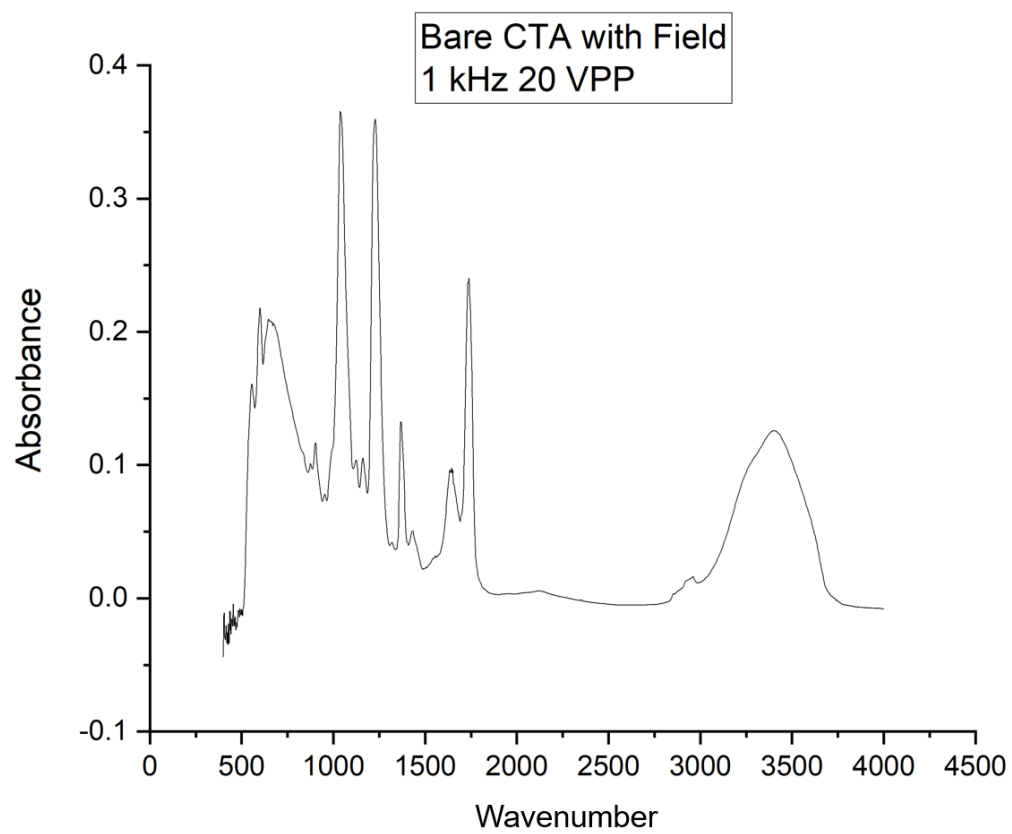


Figure 22: FTIR analysis of bare CTA membrane exposed to 1 kHz, 20 V_{p-p} AC electric field.

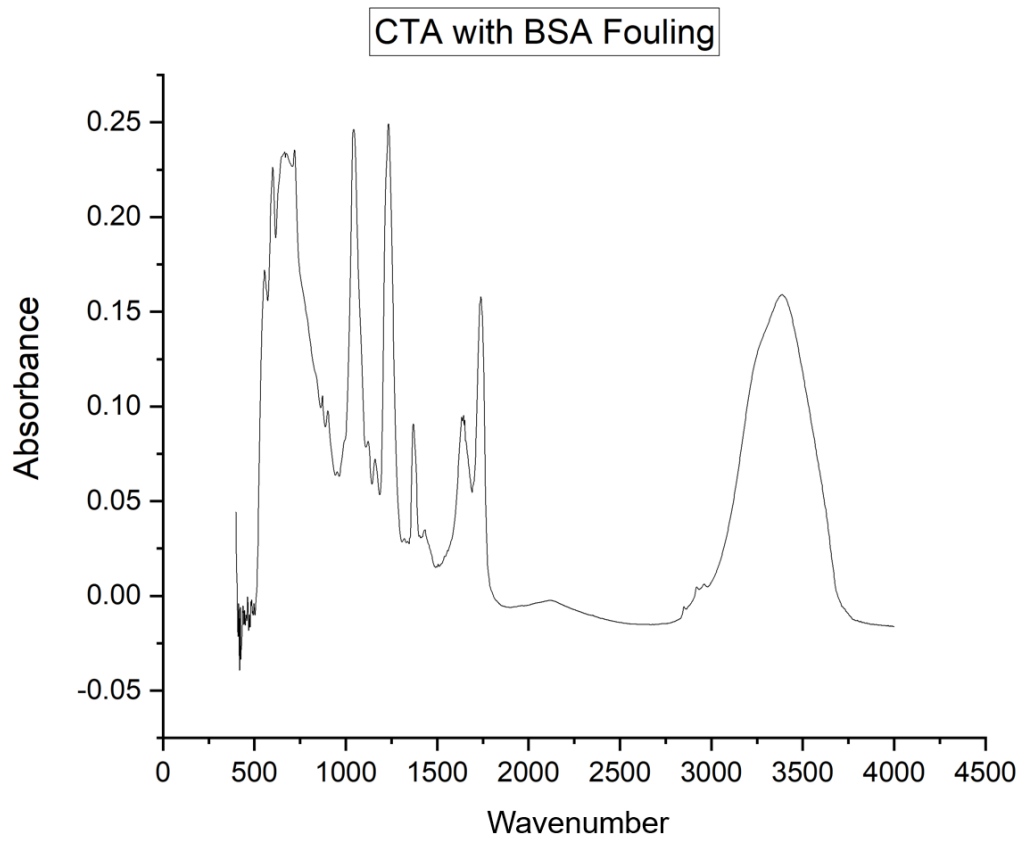


Figure 23: FTIR analysis of CTA membrane fouled with BSA at 200 mg/L with 0.5 mM CaCl₂.

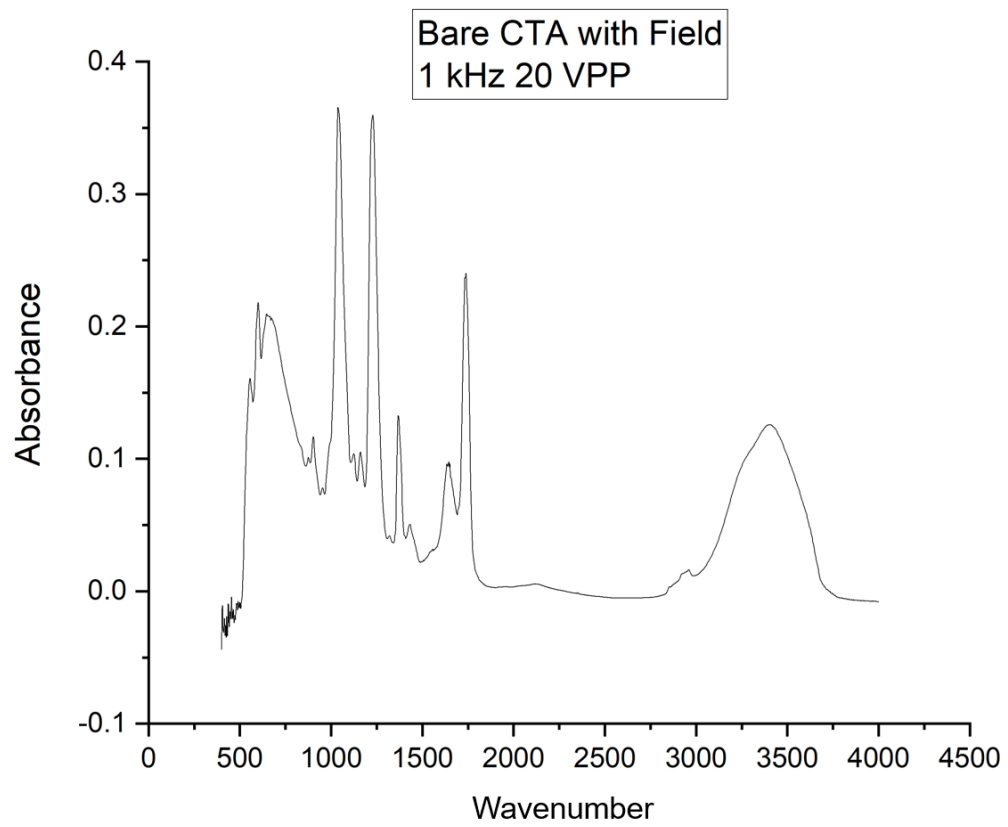


Figure 24: FTIR analysis of CTA membrane fouled with 200 mg/L BSA with 0.5 mM CaCl₂ treated with a 1 kHz, 20 V_{p-p} AC electric field.

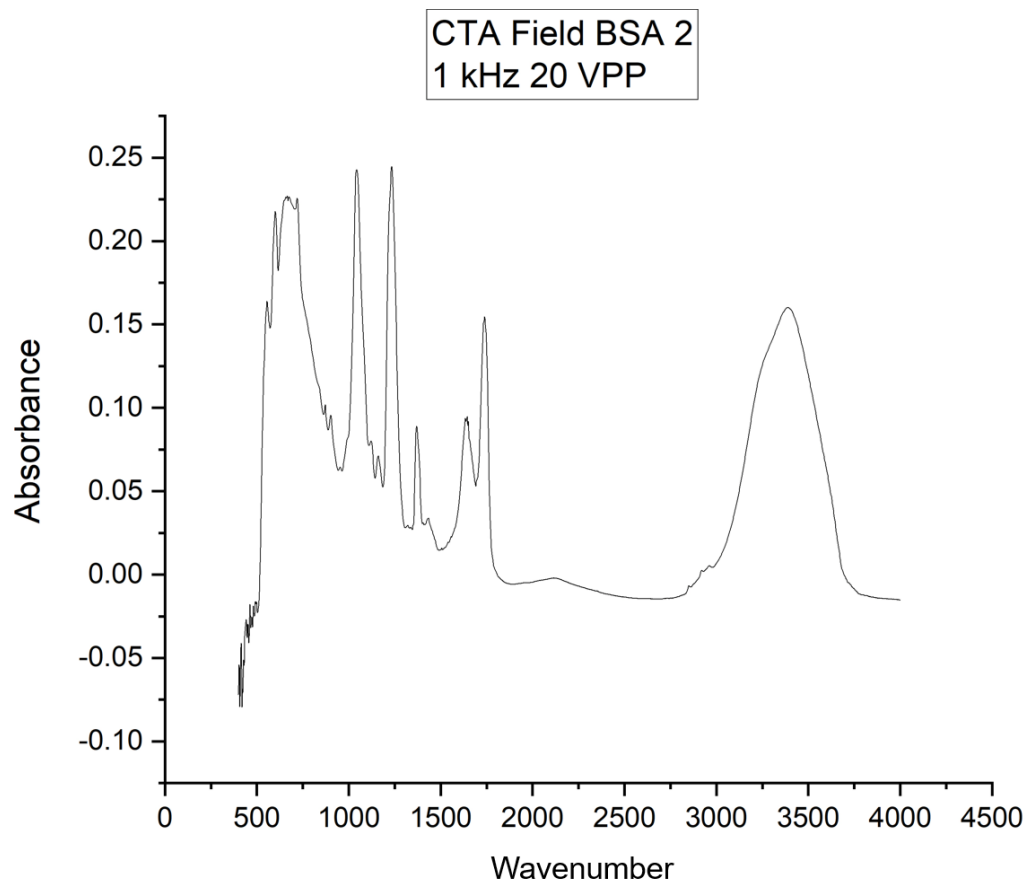


Figure 25: FTIR analysis of CTA membrane fouled with 200 mg/L BSA with 0.5 mM CaCl₂ treated with a 1 kHz, 20 V_{p-p} AC electric field.

Results from the FTIR analysis depict the absorbance of infrared radiation versus the wavelength observed by the instrument. Figure 21 depicting the FTIR spectra of bare CTA analysis is used as a baseline for this analysis. CTA FTIR analysis is identified by several peaks occurring at wavelengths between 750 and 2000, followed by a broader peak at around 3500. The analysis of the bare CTA membrane after exposure to the field yields the same spectrum, indicating no significant chemical changes have occurred on the membrane surface. All three CTA membrane samples fouled with BSA show similar peaks, however at lesser intensity in terms of absorbance due to the CTA material being

blocked by BSA foulant material. Limited conclusions are able to be drawn from this data due aside from confirmation that no significant chemical changes have occurred to the membrane material after exposure to the electric field. Furthermore, BSA spectra generally yields intense peaks between 1000 and 2000 wavelengths, with absorbance readings closer to 0.6. It is believed that the BSA foulant material could have not been fully detected by the FTIR device, and therefore no conclusions should be drawn from the resulting analysis.

7.5 Conclusions

SEM, AFM, and FTIR analysis were used to characterize differences in foulant layer composition and topography on the membrane surface. However, the procedure for SEM imaging proved unfeasible for imaging of foulant material due to the process of freeze drying via liquid nitrogen. AFM analysis samples were unable to be used due to complications during the sampling and imaging process. Limited FTIR samples were analyzed due to COVID-19 shutdowns. However, FTIR analysis did indicate that no significant changes to the chemical composition of the membrane occurred, indicating the effect of the electric field was mostly caused oscillation among the foulant molecules, which resulted in organic fouling mitigation.

Chapter 8: Conclusions

8.1 Summary of Data

Throughout this study, three different electrical fields were tested for the potential of an in-situ fouling mitigation technique for organic fouling materials using commercially available FO membranes. Bovine serum albumin and sodium alginate were used as model foulants, and the field strengths used were 100 Hz, 1 kHz, and 10 kHz set at 20 V_{p-p} for each experiment. Clean water filtration with no foulant in the feed solution was performed to serve as a baseline for all filtration trials. Fouling trials were conducted by allowing the membrane to foul completely and was used as a comparison to experiments with the electric field to test for the potential of fouling mitigation. Membrane characterization was attempted using SEM, AFM, and FTIR Spectroscopy.

This work included designing a custom-made filtration device for the purpose of propagating an electric field perpendicular through the filtration channel. This task was successfully completed, and the cell calibrated for use in all filtration trials. Overall, baseline filtration trials yielded similar results for clean water filtration and baseline fouling trials to previously published literature.

Flux data from trials using 1 g/L BSA, 200 mg/L BSA with 0.5 mM $CaCl_2$, and 200 mg/L alginate with 0.5 mM $CaCl_2$ all provide indication that AC electric fields could be used as an anti-fouling method in the forward osmotic process. Trials conducted with 100 Hz and 10 kHz indicate that at these specific frequencies and voltage, a constant AC electric field has a stronger effect on the behavior of fouling in BSA and alginate than pulsed fields. In the 1 kHz setting, however, the pulse field proved to be more effective for both BSA and alginate. Data obtained from the FTIR comparing the bare CTA membrane to a bare

CTA membrane exposed to the electric field provides an indication that the main effect of the electric field is in the fouling material themselves, causing an oscillation in these molecules that cause them to be removed from the membrane surface. No other reasonable conclusions were able to be drawn from AFM or FTIR analysis.

8.2 Limitations in Research

This project experienced interruptions during the later phases of research due to laboratory closures induced by the COVID-19 Pandemic. First and foremost, the laboratory itself was closed for an extended period of time which prevented data collection for the majority of 2020. In addition to the primary lab experiencing closure, other labs on the University of Vermont campus were closed or had severely limited availability for testing. This caused increased wait times for various procedures, or a lack of access to tests in general.

The main affect of lab closures can be seen in the effort to run AFM and FTIR analysis. Limited availability to these pieces of equipment resulted in some samples having to wait extended periods before testing, which, in the case of membrane samples, caused deterioration to the sample itself. Furthermore, some samples were inadvertently moved to a cold storage unit with a temperature set point that resulted in freezing and cracking of the membrane samples.

8.3 Future Research Possibilities

Further research working with AC fields as an anti-fouling method would benefit the current state of forward osmosis. As fouling is one of the main obstacles for any membrane process, the ability to mitigate this occurrence during operation provides a great benefit for membrane operating systems in general. It should also be emphasized that this

research mainly served as an initial investigation and proof of concept for this method of AC electric field fouling mitigation. The device used was a crude and simple prototype, and the collection of electric fields was limited. Furthermore, the foulants used represent a small fraction of all foulants present in natural and industrial waters, and the effect of AC fields on other foulants such as inorganic material or biological material should be investigated. Lastly, the membrane material used was a commercially available.

Improving upon the current prototype used in this research could help to provide a better working product to implement this process. Rectangular channel filtration cells are not optimized for maximum flux production but are the simplest and easiest to produce for lab scale studies. A hollow fiber or spiral bound membrane module designed to implement this process would provide a better real-world prototype with which to test this product and deliver maximum water recovery in tandem.

Expanding upon the foulant material used in this study would provide researchers with a better idea of which real world processes this method could be implemented. Studying a broader range of organic and biological foulants would give an indication on the usefulness in municipal water treatment processes. Expanding this current research to include biological material such as bacteria and viruses would also greatly benefit this area of study for implementing this type of device as an emergency water recovery option in developing countries. Applying this technique to inorganic foulants would mimic an industrial waste process, an area where membrane filtration is widely implemented.

Lastly, it is heavily recommended this research be expanded to the process of reverse osmosis. RO is already one of the most widely used membrane processes, but it is

greatly inhibited by fouling. Studying the potential for AC fields to mitigate fouling in RO would also greatly improve the area of membrane science in general.

Chapter 9: References

- [1] UN-Water. (n.d.). “Scarcity: UN-Water.” *UN*, United Nations, <<https://www.unwater.org/water-facts/scarcity/>> (Mar. 2020).
- [2] Badireddy, A. R., Grunert, R., and Sobel, D. (2017). “A low-cost Electro-Forward and -Reverse Osmosis Device for Production of Sterile Saline and Ultrapure Water.” University of Vermont Department of Surgery Internal Funding Grant Proposal.
- [3] “Osmosis, Tonicity, and Hydrostatic Pressure.” (n.d.). *Osmosis, Tonicity, and Hydrostatic Pressure*, Colorado State University, <<http://www.vivo.colostate.edu/hbooks/pathphys/topics/osmosis.html>> (Mar. 2020).
- [4] “Membrane Separation.” (n.d.). *EPA*, Environmental Protection Agency, <<https://iaspub.epa.gov/tdb/pages/treatment/treatmentOverview.do?treatmentProcessId=-2103528007>> (Mar. 2020).
- [5] Altaee, A., Zaragoza, G., and Tonningen, H. R. V. (2014). “Comparison between Forward Osmosis-Reverse Osmosis and Reverse Osmosis processes for seawater desalination.” *Desalination*, 336, 50–57.
- [6] Akther, N., Sodiq, A., Giwa, A., Daer, S., Arafat, H., and Hasan, S. (2015). “Recent advancements in forward osmosis desalination: A review.” *Chemical Engineering Journal*, 281, 502–522.
- [7] Yu, Y., Lee, S., and Maeng, S. K. (2016). “Forward osmosis membrane fouling and cleaning for wastewater reuse.” *Journal of Water Reuse and Desalination*, 7(2), 111–120.
- [8] Lee, S., Boo, C., Elimelech, M., and Hong, S. (2010). “Comparison of fouling behavior in forward osmosis (FO) and reverse osmosis (RO).” *Journal of Membrane Science*, 365(1-2), 34–39.
- [9] Avlonitis, S. A., Kouroumbas, K., and Vlachakis, N. (2003). “Energy consumption and membrane replacement cost for seawater RO desalination plants.” *Desalination*, Elsevier, <<https://www.sciencedirect.com/science/article/pii/S0011916403003953>> (Mar. 2020).
- [10] Singh, N., Dhiman, S., Basu, S., Balakrishnan, M., Petrinic, I., and Helix-Nielsen, C. (2019). “Dewatering of sewage for nutrients and water recovery by Forward Osmosis (FO) using divalent draw solution.” *Journal of Water Process Engineering*, Elsevier, <<https://www.sciencedirect.com/science/article/pii/S2214714419300844>> (Mar. 2020).
- [11] Xiang, X., Zou, S., and He, Z. (2016). “Energy consumption of water recovery from wastewater in a submerged forward osmosis system using commercial liquid fertilizer as a draw solute.” *Separation and Purification Technology*, Elsevier, <<https://www.sciencedirect.com/science/article/pii/S1383586616307687>> (Mar. 2020).
- [12] Lutzmiah, K., Cornelissen, E. R., Harmsen, D. J. H., Post, J. W., Lampi, K., Ramaekers, H., Rietveld, L. C., and Roest, K. (2011). “Water recovery from sewage using forward osmosis.” *Water science and technology : a journal of the International Association on Water Pollution Research*, U.S. National Library of Medicine, <<https://www.ncbi.nlm.nih.gov/pubmed/22179641>> (Mar. 2020).

- [13] Chun, Y., Mulcahy, D., Zou, L., and Kim, I. (2017). "A Short Review of Membrane Fouling in Forward Osmosis Processes." *Membranes*, 7(2), 30.
- [14] Fan, X., Liu, Y., Quan, X., and Chen, S. (2018). "Highly Permeable Thin-Film Composite Forward Osmosis Membrane Based on Carbon Nanotube Hollow Fiber Scaffold with Electrically Enhanced Fouling Resistance." *Environmental Science & Technology*, 52(3), 1444–1452.
- [15] Zumbusch, P. v, Kuleke, W., and Brunner, G. (1998). "Use of alternating electrical fields as anti-fouling strategy in ultrafiltration of biological suspensions – Introduction of a new experimental procedure for crossflow filtration." *Journal of Membrane Science*, Elsevier, <<https://www.sciencedirect.com/science/article/pii/S0376738897003104>> (Feb. 7, 2020).
- [16] Qasim, M., Darwish, N. A., Sarp, S., and Hilal, N. (2015). "Water desalination by forward (direct) osmosis phenomenon: A comprehensive review." Elsevier, *Desalination*, <<https://www.sciencedirect.com/science/article/abs/pii/S0011916415300242>> (Apr. 10, 2021).
- [17] Blandin G;Verliefde AR;Comas J;Rodriguez-Roda I;Le-Clech P; (2016). "Efficiently Combining Water Reuse and Desalination through Forward Osmosis-Reverse Osmosis (FO-RO) Hybrids: A Critical Review." U.S. National Library of Medicine, *Membranes*, <<https://pubmed.ncbi.nlm.nih.gov/27376337/>> (Apr. 10, 2021).
- [18] (2020). *Global Water Desalination Equipment Market Report, 2020-2027*, <<https://www.grandviewresearch.com/industry-analysis/water-desalination-equipment-market>> (Apr. 10, 2021).
- [19] Missimer, T. M., and Maliva, R. G. (2017). "Environmental issues in seawater reverse osmosis desalination: Intakes and outfalls." Elsevier, *Desalination*, <<https://www.sciencedirect.com/science/article/pii/S0011916417307750>> (Apr. 10, 2021).
- [20] Ly, Q. V., Hu, Y., Li, J., Cho, J., and Hur, J. (2019). "Characteristics and influencing factors of organic fouling in forward osmosis operation for wastewater applications: A comprehensive review." *Environment International*, Pergamon, <<https://www.sciencedirect.com/science/article/pii/S0160412019308050>> (Apr. 10, 2021).
- [21] Nasr, P., and Sewilam, H. (2015). "Forward osmosis: an alternative sustainable technology and potential applications in water industry." *Clean Technologies and Environmental Policy*, Springer Berlin Heidelberg, <<https://link.springer.com/article/10.1007/s10098-015-0927-8>> (Apr. 10, 2021).
- [22] Lutchmiah, K., Cornelissen, E. R., Harmsen, D. J. H., Post, J. W., Lampi, K., Ramaekers, H., Rietveld, L. C., and Roest, K. (2011). "Water recovery from sewage using forward osmosis." *Water science and technology : a journal of the International Association on Water Pollution Research*, U.S. National Library of Medicine, <<https://www.ncbi.nlm.nih.gov/pubmed/22179641/>> (Apr. 10, 2021).
- [23] Liu, X., Wu, J., Hou, L.-an, and Wang, J. (2019). "Fouling and cleaning protocols for forward osmosis membrane used for radioactive wastewater treatment." *Nuclear Engineering and Technology*, Elsevier, <<https://www.sciencedirect.com/science/article/pii/S1738573319302347#sec2>> (Apr. 10, 2021).
- [24] Mi, B., and Elimelech, M. (2008). "Chemical and physical aspects of organic fouling of forward osmosis membranes." *Journal of Membrane Science*, Elsevier, <<https://www.sciencedirect.com/science/article/abs/pii/S0376738808003219>> (Apr. 10, 2021).

- [25] Yadav, S., Ibrar, I., Bakly, S., Khanafer, D., Altaee, A., Padmanaban, V. C., Samal, A. K., and Hawari, A. H. (2020). "Organic Fouling in Forward Osmosis: A Comprehensive Review." MDPI, Multidisciplinary Digital Publishing Institute, <<https://www.mdpi.com/2073-4441/12/5/1505>> (Apr. 10, 2021).
- [26] Tow, E. W., Warsinger, D. M., Trueworthy, A. M., Swaminathan, J., Thiel, G. P., Zubair, S. M., Myerson, A. S., and V, J. H. L. (2018). "Comparison of fouling propensity between reverse osmosis, forward osmosis, and membrane distillation." *Journal of Membrane Science*, Elsevier, <<https://www.sciencedirect.com/science/article/pii/S0376738818303247>> (Apr. 10, 2021).
- [27] Moulik, S. P., Cooper, F. C., and Bier, M. (2004). "Forced-flow electrophoretic filtration of clay suspensions: Filtration in an electric field." *Journal of Colloid and Interface Science*, Academic Press, <<https://www.sciencedirect.com/science/article/pii/S0021979767902408>> (Apr. 11, 2021).
- [28] Bazant, M. Z. (2008). "AC Electro-osmotic Flow." Department of Mathematics and Institute of Soldier Nanotechnologies, Massachusetts Institute of Technology, Cambridge, MA 02139 USA, Massachusetts Institute of Technology, <http://web.mit.edu/bazant/www/papers/pdf/Bazant_2008_Ency_Microflu_Nanoflu_2.pdf>.
- [29] "Synthesis of an electrically cleanable forward osmosis membrane." (2014). Taylor & Francis, <<https://www.tandfonline.com/doi/full/10.1080/19443994.2014.978390>> (Apr. 11, 2021).
- [30] Kim, Y., Li, S., and Ghaffour, N. (2019). "Evaluation of different cleaning strategies for different types of forward osmosis membrane fouling and scaling." *Journal of Membrane Science*, Elsevier, <<https://www.sciencedirect.com/science/article/pii/S0376738819327425>> (Apr. 11, 2021).
- [31] Choi, H.-gyu, Son, M., Yoon, S. H., Celik, E., Kang, S., Park, H., Park, C. H., and Choi, H. (2015). "Alginate fouling reduction of functionalized carbon nanotube blended cellulose acetate membrane in forward osmosis." *Chemosphere*, Pergamon, <<https://www.sciencedirect.com/science/article/pii/S0045653515004609>> (Apr. 11, 2021).
- [32] Robinson, C. W., Siegel, M. H., Condemine, A., Fee, C., Fahidy, T. Z., and Glick, B. R. (2001). "Pulsed-electric-field crossflow ultrafiltration of bovine serum albumin." *Journal of Membrane Science*, Elsevier, <<https://www.sciencedirect.com/science/article/pii/S037673889385145M>> (Apr. 11, 2021).
- [33] "FTSH2O Flat Sheet Membrane, CTA, FO, CF042, 5/Pk." (n.d.). Sterlitech Corporation, FTSH2O, <<https://www.sterlitech.com/ftsh2o-flat-sheet-membrane-cta-fo-cf042-5-pk.html>> (Apr. 11, 2021).
- [34] "OsmoF2O™ Industrial." (n.d.). FLUID TECHNOLOGY SOLUTIONS, INC., <<http://ftsh2o.com/products/osmof2o-industrial/>> (Apr. 11, 2021).
- [35] "Sigracet 29 BC." (n.d.). Fuel Cell Store, <<https://www.fuelcellstore.com/sigracet-29bc>> (Apr. 11, 2021).
- [36] "Bovine Serum Albumin Market." (n.d.). Market Research Firm, <<https://www.marketsandmarkets.com/Market-Reports/bovine-serum-albumin-market-20219222.html>> (Apr. 11, 2021).

- [37] “Fouling of forward osmosis membrane by protein (BSA): effects of pH, calcium, ionic strength, initial permeate flux, membrane orientation and foulant composition.” (n.d.). Taylor & Francis, <https://www.tandfonline.com/doi/full/10.1080/19443994.2015.1060539> (Apr. 11, 2021).
- [38] Topală, T., Bodoki, A., Oprean, L., and Oprean, R. (2014). “Bovine Serum Albumin Interactions with Metal Complexes.” *Clujul medical* (1957), Iuliu Hatieganu University of Medicine and Pharmacy, <https://www.ncbi.nlm.nih.gov/pmc/articles/PMC4620676/#:~:text=Bovine%20serum%20albumin%20structure%20and%20biological%20functions&text=The%20BSA%20molecule%20consists%20of,of%2066400%20Da%20%5B1%5D.> (Apr. 11, 2021).
- [39] Westgate, P. J. (2009). University of Massachusetts Amherst ScholarWorks@UMass Amherst, University of Massachusetts Amherst, <https://scholarworks.umass.edu/cgi/viewcontent.cgi?referer=&httpsredir=1&article=1042&context=cee_ewre>
- [40] Westgate, P. J., and Park, C. (2010). “Evaluation of Proteins and Organic Nitrogen in Wastewater Treatment Effluents.” University of Massachusetts Amherst, American Chemical Society, <https://pubs.acs.org/doi/pdf/10.1021/es100244s>
- [41] “Albumin from Bovine Serum Product Information.” (n.d.). Sigma, <https://www.sigmaaldrich.com/technical-documents/articles/biology/albumin-from-bovine-serum.html> (Apr. 11, 2021).
- [42] Bank, R. C. S. B. P. D. (n.d.). “3V03: Crystal structure of Bovine Serum Albumin.” RCSB PDB, <https://www.rcsb.org/structure/3V03> (Apr. 11, 2021).
- [43] Hecht, H., and Srebnik, S. (2016). “Structural Characterization of Sodium Alginate and Calcium Alginate.” American Chemical Society, Biomacromolecules, <https://pubs.acs.org/doi/pdf/10.1021/acs.biomac.6b00378>
- [44] Motsa, M. M., Mamba, B. B., D’Haese, A., Hoek, E. M. V., and Verliefde, A. R. D. (2014). “Organic fouling in forward osmosis membranes: The role of feed solution chemistry and membrane structural properties.” *Journal of Membrane Science*, Elsevier, <https://www.sciencedirect.com/science/article/abs/pii/S0376738814001598> (Apr. 11, 2021).
- [45] “Sodium alginate.” (n.d.). National Center for Biotechnology Information. PubChem Compound Database, U.S. National Library of Medicine, <https://pubchem.ncbi.nlm.nih.gov/compound/Sodium-alginate> (Apr. 11, 2021).
- [46] Herron, J. (2005). “US7445712B2 - Asymmetric forward osmosis membranes.” Google Patents, Google, <https://patents.google.com/patent/US7445712B2/en> (Apr. 11, 2021).
- [47] Wang, Y., Zhang, M., Liu, Y., Xiao, Q., and Xu, S. (2016). “Quantitative evaluation of concentration polarization under different operating conditions for forward osmosis process.” *Desalination*, Elsevier, <https://www.sciencedirect.com/science/article/abs/pii/S0011916416308529> (Apr. 11, 2021).
- [48] Swapp, S. (2017). “Scanning Electron Microscopy (SEM).” Techniques, <https://serc.carleton.edu/research_education/geochemsheets/techniques/SEM.html> (Apr. 11, 2021).

- [49] Huang, L., and McCutcheon, J. R. (2015). "Impact of support layer pore size on performance of thin film composite membranes for forward osmosis." *Journal of Membrane Science*, Elsevier, <<https://www.sciencedirect.com/science/article/abs/pii/S0376738815000411>> (Apr. 11, 2021).
- [50] Mai, W. (n.d.). *Fundamental Theory of Atomic Force Microscopy*, <<http://www.nanoscience.gatech.edu/zlwang/research/afm.html>> (Apr. 11, 2021).
- [51] "FTIR Spectroscopy Basics: Thermo Fisher Scientific - US." (n.d.). FTIR Spectroscopy Basics | Thermo Fisher Scientific - US, <<https://www.thermofisher.com/us/en/home/industrial/spectroscopy-elemental-isotope-analysis/spectroscopy-elemental-isotope-analysis-learning-center/molecular-spectroscopy-information/ftir-information/ftir-basics.html>> (Apr. 11, 2021).
- [52] Mehta, D., Gupta, L., and Dhingra, R. (2014). "Forward Osmosis in India: Status and Comparison with Other Desalination Technologies." *International Scholarly Research Notices*, Hindawi, <<https://www.hindawi.com/journals/isrn/2014/175464/>> (Apr. 11, 2021).
- [53] Motsa, M. M., Mamba, B. B., D'Haese, A., Hoek, E. M. V., and Verliefde, A. R. D. (2014). "Organic fouling in forward osmosis membranes: The role of feed solution chemistry and membrane structural properties." *Journal of Membrane Science*, Elsevier, <<https://www.sciencedirect.com/science/article/abs/pii/S0376738814001598>> (Apr. 11, 2021).
- [54] Xie, M., Lee, J., Nghiem, L. D., and Elimelech, M. (2015). "Role of pressure in organic fouling in forward osmosis and reverse osmosis." *Journal of Membrane Science*, Elsevier, <<https://www.sciencedirect.com/science/article/abs/pii/S0376738815300600#:~:text=Our%20findings%20suggest%20that%20pressure,driving%20force%20is%20hydraulic%20pressure.>> (Apr. 11, 2021).
- [55] Avlonitis, S. A., Kouroumbas, K., and Vlachakis, N. (2003). "Energy consumption and membrane replacement cost for seawater RO desalination plants." *Desalination*, Elsevier, <<https://www.sciencedirect.com/science/article/abs/pii/S0011916403003953>> (Apr. 11, 2021).
- [56] Wang, L., Li, T., Chu, H., Zhang, W., Huang, W., Dong, B., Wu, D., and Chen, F. (2021). "Natural organic matter separation by forward osmosis: Performance and mechanisms." *Water Research*, Pergamon, <<https://www.sciencedirect.com/science/article/pii/S0043135421000270>> (Apr. 11, 2021).
- [57] Nguyen, T., Roddick, F. A., and Fan, L. (2012). "Biofouling of water treatment membranes: a review of the underlying causes, monitoring techniques and control measures." *Membranes*, MDPI, <<https://www.ncbi.nlm.nih.gov/pmc/articles/PMC4021920/>> (Apr. 11, 2021).
- [58] Reclamation, B. of. (2016). "Forward Osmosis Evaluation and Applications for Reclamation." Bureau of Reclamation : Research and Development | Research and Development Office, Bureau of Reclamation, <<https://www.usbr.gov/research/projects/detail.cfm?id=7911>> (Apr. 11, 2021).
- [59] Jagannadh, S. N., and Muralidhara, M. S. (1996). "Electrokinetics Methods To Control Membrane Fouling." American Chemical Society, <<https://pubs.acs.org/doi/10.1021/ie9503712>>
- [60] Coday, Bryan & Yaffe, Bethany & Xu, Pei & Cath, Tzahi. (2014). Rejection of Trace Organic Compounds by Forward Osmosis Membranes: A Literature Review. *Environmental science & technology*. 48. 10.1021/es4038676.

[61] Lee, H.-J., Moon, S.-H., and Tsai, S.-P. (2002). "Effects of pulsed electric fields on membrane fouling in electrodialysis of NaCl solution containing humate." *Separation and Purification Technology*, Elsevier, <<https://www.sciencedirect.com/science/article/abs/pii/S1383586601001678>> (Apr. 11, 2021).

[62] "Cellulose triacetate." (n.d.). National Center for Biotechnology Information. PubChem Compound Database, U.S. National Library of Medicine, <<https://pubchem.ncbi.nlm.nih.gov/compound/Cellulose-triacetate>> (Apr. 11, 2021).

[63] Wang, X., Zhao, Y., Yuan, B., Wang, Z., Li, X., and Ren, Y. (2015). "Comparison of biofouling mechanisms between cellulose triacetate (CTA) and thin-film composite (TFC) polyamide forward osmosis membranes in osmotic membrane bioreactors." *Bioresource Technology*, Elsevier, <<https://www.sciencedirect.com/science/article/pii/S096085241501620X>> (Apr. 11, 2021).

[64] Gu, Y., Wang, Y.-N., Wei, J., and Tang, C. Y. (2013). "Organic fouling of thin-film composite polyamide and cellulose triacetate forward osmosis membranes by oppositely charged macromolecules." *Water Research*, Pergamon, <<https://www.sciencedirect.com/science/article/pii/S0043135413000250>> (Apr. 11, 2021).

[65] Li, G., Li, X.-M., He, T., Jiang, B., and Gao, C. (n.d.). "Cellulose triacetate forward osmosis membranes: preparation and characterization." Taylor & Francis, <<https://www.tandfonline.com/doi/full/10.1080/19443994.2012.749246?needAccess=rue>> (Apr. 11, 2021).

[66] "Sepa Cell, Crossflow, 34 mil Channel Depth, Electrode Modified, Acrylic." (n.d.). Sterlitech Corporation, <<https://www.sterlitech.com/sepa-cell-crossflow-34-mil-channel-depth-electrode-modified-acrylic.html>> (Apr. 11, 2021).

[67] "Albumin from Bovine Serum Product Information." (n.d.). Sigma, <<https://www.sigmaaldrich.com/technical-documents/articles/biology/albumin-from-bovine-serum.html>> (Apr. 11, 2021).

[68] Yu, D. (2012). "Evaluation of effluent organic nitrogen and its impacts on receiving water bodies." University of Massachusetts Amherst ScholarWorks@UMass Amherst, University of Massachusetts Amherst, <https://scholarworks.umass.edu/cgi/viewcontent.cgi?article=1040&context=cee_ewre>